Journal of Sound and Vibration 363 (2016) 473–494

Contents lists available at ScienceDirect

Journal of Sound and Vibration

journal homepage: www.elsevier.com/locate/jsvi

Multi-modal vibration amplitudes of taut inclined cables due to direct and/or parametric excitation

J.H.G. Macdonald *

Department of Civil Engineering, University of Bristol, Queen's Building, University Walk, Bristol BS8 1TR, UK

ARTICLE INFO

Article history:
Received 19 September 2014
Received in revised form
3 November 2015
Accepted 6 November 2015
Handling Editor: W. Lacarbonara
Available online 21 November 2015

Keywords:
Cable dynamics
Inclined cables
Parametric excitation
Nonlinear vibrations
Multi-mode model
Modal coupling
Cable sag

ABSTRACT

Cables are often prone to potentially damaging large amplitude vibrations. The dynamic excitation may be from external loading or motion of the cable ends, the latter including direct excitation, normally from components of end motion transverse to the cable, and parametric excitation induced by axial components of end motion causing dynamic tension variations. Geometric nonlinearity can be important, causing stiffening behaviour and nonlinear modal coupling. Previous analyses of the vibrations, often neglecting sag, have generally dealt with direct and parametric excitation separately or have reverted to numerical solutions of the responses. Here a nonlinear cable model is adopted, applicable to taut cables such as on cable-stayed bridges, that allows for cable inclination, small sag (such that the vibration modes are similar to those of a taut string), multiple modes in both planes and end motion and/or external forcing close to any natural frequency. Based on the method of scaling and averaging it is found that, for sinusoidal inputs and positive damping, non-zero steady state responses can only occur in the modes in each plane with natural frequencies close to the excitation frequency and those with natural frequencies close to half this frequency. Analytical solutions, in the form of non-dimensional polynomial equations, are derived for the steady state vibration amplitudes in up to three modes simultaneously: the directly excited mode, the corresponding nonlinearly coupled mode in the orthogonal plane and a parametrically excited mode with half the natural frequency. The stability of the solutions is also identified. The outputs of the equations are consistent with previous results, where available. Example results from the analytical solutions are presented for a typical inclined bridge cable subject to vertical excitation of the lower end, and they are validated by numerical integration of the equations of motion and against some previous experimental results. It is shown that the modal interactions and sag (although very small) affect the responses significantly.

1. Introduction

Cables are used as structural elements in various contexts at various scales and are often prone to quite large transverse vibrations due to their low inherent damping. Cable dynamics can be complex and has attracted extensive research, especially regarding the effects of geometric nonlinearities, as reviewed by Nayfeh and Pai [1], Rega [2,3] and Ibraim [4]. The dynamic behaviour of cables is greatly influenced by the static sag, as addressed by Irvine and Caughey [5] and quantified by

* Tel.: +44 117 331 5735.
E-mail address: john.macdonald@bristol.ac.uk

http://dx.doi.org/10.1016/j.jsv.2015.11.012
0022-460X/

Irvine's parameter λ^2, whereby the sag increases the natural frequencies in the plane of the sag (in-plane) relative to those of a taut string or the cable in the out-of-plane direction. Much of the past research has been on taut strings (i.e. no sag, $\lambda^2=0$) or cables in the crossover regions, the first of which occurs when $\lambda^2=4\pi^2$. At crossovers the natural frequency of an odd (symmetric) in-plane mode has been increased sufficiently by the sag that it equals that of an even (anti-symmetric) mode in each plane, leading to strong modal interactions [6–9]. This situation is relevant to cables with significant sag such as electricity transmission lines. In contrast this paper deals with the vibration amplitudes of taut cables, i.e. those with very small sag (of which taut strings are a special case), with $\lambda^2 \leq O(1)$. This applies, for example, to the inclined cables of cable-stayed bridges. For these cables the natural frequencies and mode shapes are close to those for a taut string, i.e. a harmonic series, the sag causing just slight detuning of the natural frequencies of the odd in-plane modes relative to the corresponding out-of-plane modes. This then leads to interactions of different combinations of modes to those for cables in the crossover regions. At crossovers there are three modes with the same natural frequency (two in-plane and one out-of-plane) and one out-of-plane mode with half the natural frequency, whereas for taut cables there are two modes (one in each plane) with close natural frequencies and, where those are even modes, two more (also one in each plane) close to half the natural frequency.

The main aim of this paper is to provide analytical solutions for the steady state amplitudes of vibrations of taut inclined cables due to harmonic planar excitation, for different combinations of modes that may be directly and/or parametrically excited and which interact with each other nonlinearly. A secondary aim is to identify how very small sag ($0<\lambda^2 \leq O(1)$) causes differences in the behaviour from that of a taut string.

Cables may be excited dynamically by external forcing, such as from wind loading, or by motion of one or both of the ends, such as from bridge deck or tower motion. Often in practice, in accordance with design guidelines [10,11], the components of end motion transverse and axial to the cable axis are considered separately, the former providing direct excitation similar to external forcing and the latter giving parametric excitation via tension variations. However, in some situations, such as in cable-stayed bridges or guyed masts, there can be cable end motion with components both axial and transverse to the cable, providing both types of excitation simultaneously. The resulting behaviour can be affected significantly by nonlinear interactions between the modal responses. Although strictly there can be dynamic interactions of the cable with the rest of the structure [12] here they are neglected and the cable end motions are prescribed, which is a reasonable representation of the behaviour when the rest of the structure is suitably massive.

For direct excitation only, of a taut string subject to harmonic planar excitation, Nayfeh and Mook [13] identified planar and non-planar steady-state solutions using the method of multiple scales. The amplitude of the planar solution was found to be unstable above a critical amplitude. Thereafter a non-planar whirling solution was stable, the amplitudes of the in-plane and out-of-plane motions being found by numerical continuation. Miles [14] similarly derived the averaged response of a 2-degree-of-freedom (2DOF) model of a taut string (one mode in each plane with the same natural frequency) subject to external direct excitation. He also considered stability of the solutions and identified Hopf bifurcations of the non-planar response. Bajaj and Johnson [15] discuss the solutions further, including periodic and chaotic solutions.

Meanwhile, considering responses to external forcing of a planar 1DOF model but allowing for sag, Benedettini and Rega [16] used a fourth order multiple time scale perturbation method to identify the steady state response amplitudes. It was shown that a suspended cable with $\lambda^2=15.36$ exhibited initial softening behaviour due to the quadratic nonlinearity and subsequent stiffening from the cubic nonlinearity, but a taut cable with $\lambda^2=1.536$ exhibited only stiffening behaviour from the cubic term, with negligible effect of the quadratic term. Later Gattulli et al. [17] compared numerical continuation of a 10-mode analytical model and numerical integration of a finite element formulation for an externally forced cable with $\lambda^2=15.36$ close to a 2:1 resonance between the natural frequencies of the third and first in-plane modes, and for a slacker cable with $\lambda^2>4\pi^2$. The two methods gave similar results and although complex modal interactions were identified it was found that only up to three low frequency modes, with certain resonant conditions, were significantly involved in the solutions. It was also found that the kinematic condensation of the longitudinal displacements in the analytical model gave no appreciable error. For cables with a larger range of Irvine's parameter, Srinil and co-authors [18,19] considered the effects of sag, inclination and kinematic condensation on modal interactions around frequency crossovers and 2:1 resonances that occur for certain values of λ^2 above 15. For such cables the inclination causes a variation in tension over the length giving an asymmetric static sag profile, leading to frequency avoidances, rather than crossovers, and gives coupling between more modes and increased significance of the longitudinal displacement than for horizontal cables. However, for taut cables the variation in tension over the length and the associated features are negligible.

For parametric excitation alone, there is zero response until the input amplitude exceeds a certain threshold, dependent on the damping, after which large amplitude transverse vibrations of the cable occur, which are affected relatively little by the damping. Different authors have calculated the stability boundaries and the amplitudes of vibrations based on the Mathieu–Hill equation for a single mode [20–22]. Uhrig [21] included nonlinear coupling terms between modes in his equations of motion but reduced them to uncoupled linear Mathieu equations to define the stability boundaries.

A situation in which both direct and parametric excitation can occur is an inclined taut cable subject to vertical or horizontal support excitation of one end, which has been considered by several authors. Cai and Chen [23] first conducted numerical simulations of the in-plane response of inclined cables to horizontal sinusoidal motion of the upper end. Nayfeh et al. [24] presented theoretical and experimental nonlinear responses of the similar system of a taut string subjected to end excitation at an angle to the cable axis. The method of multiple scales and a numerical continuation technique were used to find steady state solutions and their stability. Resonant responses were found in up to three modes; the directly excited

mode, the paired mode in the other plane, and a parametrically excited mode with half the natural frequency. The predicted responses agreed well with experimental measurements. Pinto da Costa et al. [25] discussed the relative importance of direct and parametric excitation of inclined taut cables by analytically considering horizontal and vertical cables and from numerical solutions of vibration amplitudes of four different inclined cables. Caswita and Van Der Burgh [26] addressed the in-plane behaviour of an inclined taut string subjected to horizontal motion of the upper end. Using the method of averaging, for a given input amplitude, they identified regions, in inclination angle-input frequency space, of different behaviour involving a directly excited mode and a parametrically excited mode. Berlioz and Lamarque [27] used the method of multiple scales to estimate the response amplitudes of a 1DOF model of the first in-plane mode of an inclined taut cable subject to support excitation around its natural frequency (direct excitation) or at twice its natural frequency (parametric excitation), obtaining good agreement with experiments after fitting parameters. Georgakis and Taylor [28,29] used numerical simulations to explore the responses of an inclined taut cable subjected to sinusoidal and stochastic support excitations, while Wang and Zhao [30] used the shooting method and the continuation technique to numerically estimate the amplitudes of planar and non-planar responses for certain cases. Although all these papers have identified interesting features in the dynamic behaviour of taut cables or taut strings to direct and parametric excitation, they have each considered limited cases and estimates of the response amplitudes have resorted to some numerical technique using certain parameter values.

For cables with very small sag, the natural frequencies are close to a harmonic series [5]. Hence for primary parametric excitation of any one mode, at twice its natural frequency, the excitation frequency is close to the natural frequency of another mode. Therefore, inputs at an angle to the cable axis (e.g. vertical end motion to an inclined cable) can cause simultaneous direct excitation and parametric excitation of at least two modes, which are nonlinearly coupled [25]. The response of the directly excited mode can modify the dynamic stability and response amplitudes of other modes. The effect on the stability boundaries was first explicitly considered by Gonzalez-Buelga et al. [31] for a 3DOF model of an inclined cable excited vertically at the lower end around the natural frequency of the second in-plane mode. The stability analysis was generalised by Macdonald et al. [32] to include all in-plane and out-of-plane modes, for excitation close to any natural frequency. Marsico et al. [33] then used numerical continuation to find steady state amplitudes, for certain parameter values, from the averaged modulation equations for the first two modes in each plane excited in-plane close to the second natural frequency.

Extending the approach of Gonzalez-Buelga et al. [31] and Macdonald et al. [32], this paper addresses the steady state vibration amplitudes of taut cables subjected to direct and/or parametric excitation. In contrast to previous studies, which have mainly presented numerical results or have just considered special cases (e.g. a taut string), analytical solutions are found, in the form of polynomials, for the general case. They allow for an infinite number of nonlinearly coupled modes in both planes, cable inclination and small sag (which slightly detunes the odd in-plane modes and modifies the effects of the excitation). Solutions, for excitation close to any natural frequency, are found for simultaneous steady state responses in up to three modes: the directly excited mode, the paired mode in the other plane (with a similar natural frequency), and a parametrically excited mode in either plane, with approximately half the natural frequency. The solutions are expressed in non-dimensional terms using physically meaningful parameters. The assumptions in the analysis are discussed in Section 2.3, the most significant of which is that the sag is very small so the detuning of the in-plane modes is only slight.

2. Theoretical model

2.1. Equations of motion

The nonlinear cable formulation from Warnitchai et al. [34] has been adopted, which is valid for elastic inclined taut cables and has been shown to match experiments [31,32,35]. The equations of motion include cubic and quadratic nonlinearities and allow for external loads and small support motions in all directions at both ends of the cable. The cable geometry is defined in Fig. 1. The static sag profile lies in the x–z plane, so z represents in-plane motion and y represents out-of-plane motion. The angle of inclination of the chord from the horizontal is θ. Axial vibrations of the cable are

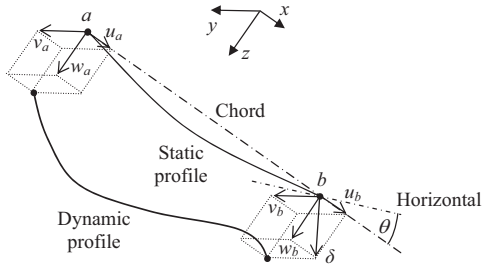

Fig. 1. Definitions of cable geometry and end motions.

neglected since they occur at much higher frequencies than transverse vibrations. Using a Galerkin model based on near-sinusoidal mode shapes, the equation of motion of the nth out-of-plane cable mode is expressed as [34]

$$m\left(\ddot{y}_n+2\xi_{yn}\omega_{yn}\dot{y}_n+\omega_{yn}^2y_n\right)+\sum_k \nu_{nk}y_n\left(y_k^2+z_k^2\right)+\sum_k 2\beta_{nk}y_nz_k$$
$$+2\eta_n(u_b-u_a)y_n+\zeta_n\left(\ddot{v}_a+(-1)^{n+1}\ddot{v}_b\right)=f_{yn} \tag{1}$$

and that of the nth in-plane cable mode as

$$m\left(\ddot{z}_n+2\xi_{zn}\omega_{zn}\dot{z}_n+\omega_{zn}^2z_n\right)+\sum_k \nu_{nk}z_n\left(y_k^2+z_k^2\right)+\sum_k 2\beta_{nk}z_nz_k$$
$$+\sum_k \beta_{kn}\left(y_k^2+z_k^2\right)+2\eta_n(u_b-u_a)z_n+\zeta_n\left(\ddot{w}_a+(-1)^{n+1}\ddot{w}_b\right)-\alpha_n(\ddot{u}_b-\ddot{u}_a)=f_{zn} \tag{2}$$

where y_n and z_n are the generalised displacements of the cable in the nth out-of-plane and in-plane modes respectively, for any n (note that the summations over modes y_k and z_k, for all k, cause nonlinear coupling between modes); subscripts a and b denote the top and bottom cable ends respectively; and the modal mass m (the same for all modes) and the parameters ν_{nk}, β_{nk}, η_n, ζ_n and α_n are given by

$$m=\frac{\rho AL}{2},\nu_{nk}=\frac{EA\pi^4n^2k^2}{8L^3},\beta_{nk}=\frac{EA\pi\gamma n^2}{4L\sigma_s}\left(\frac{1+(-1)^{k+1}}{k}\right),$$
$$\eta_n=\frac{E_qA\pi^2n^2}{4L^2},\zeta_n=\frac{\rho AL}{n\pi},\alpha_n=\frac{\rho AL}{n^3\pi^3}\frac{\gamma LE_q}{\sigma_s^2}\left(1+(-1)^{n+1}\right),$$

where ρ is the density, A the cross sectional area, L the chord length, E Young's Modulus and σ_s the static stress.

Based on a very low sag approximation, Ernst's equivalent modulus of the cable, E_q [36], Irvine's non-dimensional sag parameter, λ^2 [5], and the component of weight normal to the cable axis, γ, are given by

$$E_q=\frac{E}{1+\lambda^2/12},\lambda^2=\frac{E}{\sigma_s}\left(\frac{\gamma L}{\sigma_s}\right)^2,\gamma=\rho g\ \cos\ \theta,$$

where g is the gravitational acceleration.

f_{yn} and f_{zn} are the generalised external loads on the cable in each mode and it is assumed that damping (including any aerodynamic damping [37]) can be modelled as viscous with modal damping ratios ξ_{zn} and ξ_{yn}.

Again based on a very low sag approximation, the out-of-plane and in-plane circular natural frequencies, ω_{yn} and ω_{zn} respectively, are given by [32]

$$\omega_{yn}=\omega_n=n\omega_1,\omega_{zn}\approx\omega_n(1+\kappa_n),$$

where $\omega_1=\frac{\pi}{L}\sqrt{\frac{\sigma_s}{\rho}}$ and $\kappa_n=\left(\frac{\lambda^2}{\pi^4n^4}\right)\left(1+(-1)^{n+1}\right)^2$.

In Eqs. (1) and (2), the m terms are linear, the ν_{nk} terms are cubic nonlinearities from stretching of the cable in the deformed shape, the β_{nk} terms are quadratic nonlinearities from the effect of the static sag (causing asymmetry of the tension variations for upwards and downwards displacements in the odd in-plane modes), the η_n terms cause parametric excitation from the axial end displacements, the ζ_n and α_n terms cause direct excitation from the end accelerations, and the f_{yn} and f_{zn} terms cause direct excitation from external forcing. Details of the derivation of the model are given by Warnitchai et al. [34].

For conciseness the support motions can be expressed as

$$u=u_b-u_a,v_n=v_a+(-1)^{n+1}v_b,w_n=w_a+(-1)^{n+1}w_b.$$

The cable is excited by prescribed sinusoidal support motions (which in general can be a combination of u, v_n and w_n components) and/or by external generalised forces f_{yn} or f_{zn}, close to the pth natural frequency, with excitation frequency

$$\Omega=p\omega_1(1+\mu)$$

where μ is a small frequency detuning parameter.

For clarity of the notation, n represents the mode number in the general case, p is the mode number of the directly excited mode, with natural frequency close to the excitation frequency, and its pair in the other plane, and, for even p, q ($\equiv p/2$) is the mode number of the modes (one in each plane) with natural frequencies close to half the excitation frequency (i.e. potentially parametrically excited modes).

2.2. General non-dimensional nonlinear equations for steady state response amplitudes

The method of scaling and averaging [38] was applied to the equations of motion, as described in [32]. Time was transformed using the relationship $\tau=(1+\mu)t$ and the small parameter ε was introduced for book-keeping purposes. The

method assumes each mode responds only near its natural frequency so the responses can be expressed as

$$y_n = y_{nc}\ \cos(\omega_n\tau) + y_{ns}\ \sin(\omega_n\tau), z_n = z_{nc}\ \cos(\omega_n\tau) + z_{ns}\ \sin(\omega_n\tau),$$

where y_{nc}, y_{ns}, z_{nc} and z_{ns} are slowly varying amplitudes of each component. Averaged derivatives of the amplitudes, represented with an additional subscript a, are, to first order ε [32] (with the external forcing terms included here for completeness):

$$y'_{nca} = -\frac{\varepsilon}{\omega_n}\left\{\xi_{yn}\omega_n^2 y_{nca} + \mu\omega_n^2 y_{nsa} - \frac{\nu_{nn}}{8m}y_{nsa}(Y_{na}^2 - Z_{na}^2) - \sum_k \frac{\nu_{nk}}{4m}y_{nsa}(Y_{ka}^2 + Z_{ka}^2) - \frac{\nu_{nn}}{4m}z_{nsa}C_{na} + \delta_{2n,p}\frac{\eta_n}{2m}Uy_{nsa}\right\}, \tag{3}$$

$$y'_{nsa} = \frac{\varepsilon}{\omega_n}\left\{-\xi_{yn}\omega_n^2 y_{nsa} + \mu\omega_n^2 y_{nca} - \frac{\nu_{nn}}{8m}y_{nca}(Y_{na}^2 - Z_{na}^2) - \sum_k \frac{\nu_{nk}}{4m}y_{nca}(Y_{ka}^2 + Z_{ka}^2) - \frac{\nu_{nn}}{4m}z_{nca}C_{na} - \delta_{2n,p}\frac{\eta_n}{2m}Uy_{nca} + \delta_{n,p}\frac{\omega_n^2}{2m}\zeta_n V_n + \delta_{n,p}\frac{1}{2m}F_{yn}\right\}, \tag{4}$$

$$z'_{nca} = -\frac{\varepsilon}{\omega_n}\left\{\xi_{zn}\omega_n^2 z_{nca} + (\mu - \kappa_n)\omega_n^2 z_{nsa} - \frac{\nu_{nn}}{8m}z_{nsa}(Z_{na}^2 - Y_{na}^2) - \sum_k \frac{\nu_{nk}}{4m}z_{nsa}(Z_{ka}^2 + Y_{ka}^2) - \frac{\nu_{nn}}{4m}y_{nsa}C_{na} + \delta_{2n,p}\frac{\eta_n}{2m}Uz_{nsa}\right\}, \tag{5}$$

$$z'_{nsa} = \frac{\varepsilon}{\omega_n}\left\{-\xi_{zn}\omega_n^2 z_{nsa} + (\mu - \kappa_n)\omega_n^2 z_{nca} - \frac{\nu_{nn}}{8m}z_{nca}(Z_{na}^2 - Y_{na}^2) - \sum_k \frac{\nu_{nk}}{4m}z_{nca}(Z_{ka}^2 + Y_{ka}^2) - \frac{\nu_{nn}}{4m}y_{nca}C_{na} - \delta_{2n,p}\frac{\eta_n}{2m}Uz_{nca} + \delta_{n,p}\frac{\omega_n^2}{2m}(\zeta_n W_n - \alpha_n U) + \delta_{n,p}\frac{1}{2m}F_{zn}\right\}, \tag{6}$$

where $Y_{na}^2 = y_{nca}^2 + y_{nsa}^2$ and $Z_{na}^2 = z_{nca}^2 + z_{nsa}^2$ are the squares of the modal amplitudes, $C_{na} = y_{nca}z_{nca} + y_{nsa}z_{nsa}$ are cross-coupling terms, $\delta_{i,j}$ is the Kronecker delta function, U, V_n and W_n are the amplitudes of the sinusoidal support motions u, v_n and w_n, F_{yn} and F_{zn} are the amplitudes of the sinusoidal external generalised forces f_{yn} and f_{zn}, and primes represent differentiation with respect to τ.

The quadratic (β_{nk}) terms in Eqs. (1) and (2) are lost in the averaging to derive Eqs. (3)–(6), due to the assumption that each mode only responds close to its own natural frequency. In practice there may be components of motion of some modes at other frequencies, which, through the Galerkin representation, could be equivalent to distortion of the actual mode shapes. However, the significance of these additional components for a typical taut cable is addressed in Section 5.

Marsico et al. [33] derived averaged equations equivalent to Eqs. (3)–(6) for the first two modes in each plane for end excitation around the second natural frequency ($p=2$), and found solutions of steady state vibration amplitudes for certain parameter values by numerical continuation. Here, in contrast, analytical solutions are found, in non-dimensional form, for any mode numbers.

The input displacement amplitudes are non-dimensionalised with respect to L: $\hat{U} = U/L$, etc., and the output displacement amplitudes are non-dimensionalised as $\tilde{y}_{nc} = y_{nca}n\pi/L$, $\tilde{Y}_n = Y_{na}n\pi/L$, etc., which, given that the mode shapes are sinusoidal, are equal to the amplitudes of cable end rotations. Two non-dimensional cable parameters are defined: $\varepsilon_s = \sigma_s/E$ (i.e. static strain) and $\Gamma = \rho g L/\sigma_s$ (i.e. ratio of cable weight to tension, the static mid-span sag normal to the chord being given by $\Gamma L\cos\theta\,/8$). The cable inclination angle, θ, and the damping ratios in each mode, ξ_{zn} and ξ_{yn}, complete the set of fundamental non-dimensional parameters. Irvine's non-dimensional sag parameter can be expressed as $\lambda^2 = \Gamma^2\cos^2\theta\,/\varepsilon_s$.

Steady state solutions of the modal response amplitudes can be found by setting the derivatives of the amplitudes to zero. Hence the above equations become, in non-dimensional form:

$$\xi_{yn}\tilde{y}_{nc} + b_{yn}\tilde{y}_{ns} - \frac{1}{16\varepsilon_s}\tilde{C}_n\tilde{z}_{ns} = -\delta_{2n,p}\frac{1}{4\varepsilon_s(1+\lambda^2/12)}\hat{U}\tilde{y}_{ns}, \tag{7}$$

$$-\xi_{yn}\tilde{y}_{ns} + b_{yn}\tilde{y}_{nc} - \frac{1}{16\varepsilon_s}\tilde{C}_n\tilde{z}_{nc} = \delta_{2n,p}\frac{1}{4\varepsilon_s(1+\lambda^2/12)}\hat{U}\tilde{y}_{nc} - \delta_{n,p}\hat{X}_{yn}, \tag{8}$$

$$\xi_{zn}\tilde{z}_{nc} + b_{zn}\tilde{z}_{ns} - \frac{1}{16\varepsilon_s}\tilde{C}_n\tilde{y}_{ns} = -\delta_{2n,p}\frac{1}{4\varepsilon_s(1+\lambda^2/12)}\hat{U}\tilde{z}_{ns}, \tag{9}$$

$$-\xi_{zn}\tilde{z}_{ns} + b_{zn}\tilde{z}_{nc} - \frac{1}{16\varepsilon_s}\tilde{C}_n\tilde{y}_{nc} = \delta_{2n,p}\frac{1}{4\varepsilon_s(1+\lambda^2/12)}\hat{U}\tilde{z}_{nc} - \delta_{n,p}\hat{X}_{zn}, \tag{10}$$

where

$$b_{yn} = \mu - \frac{1}{32\varepsilon_s}\left\{(\tilde{Y}_n^2 - \tilde{Z}_n^2) + 2\sum_k (\tilde{Y}_k^2 + \tilde{Z}_k^2)\right\} \tag{11a}$$

$$b_{zn} = \mu - \kappa_n - \frac{1}{32\varepsilon_s}\left\{(\tilde{Z}_n^2 - \tilde{Y}_n^2) + 2\sum_k (\tilde{Y}_k^2 + \tilde{Z}_k^2)\right\} \tag{11b}$$

$$\hat{X}_{yn} = \hat{V}_n + \frac{n\pi F_{yn}}{\rho A L^2 \omega_n^2} \tag{11c}$$

$$\hat{X}_{zn} = \hat{W}_n - \left(1 + (-1)^{n+1}\right)\frac{\Gamma\ \cos\ \theta}{\pi^2 n^2 \varepsilon_s (1 + \lambda^2/12)}\hat{U} + \frac{n\pi F_{zn}}{\rho A L^2 \omega_n^2} \tag{11d}$$

Hence there are 4 nonlinear algebraic equations in the 4 modal amplitude variables, $\tilde{y}_{nc}$, $\tilde{y}_{ns}$, $\tilde{z}_{nc}$ and $\tilde{z}_{ns}$, for each mode number, n.

b_{yn} and b_{zn} include nonlinear coupling terms between modes, as does $\tilde{C}_n$. The equations for the in-plane modes (Eqs. (9) and (10)) are identical to those for the out-of-plane modes (Eqs. (7) and (8)) except that all occurrences of y and z are interchanged, b_{zn} includes κ_n, representing the detuning of odd in-plane natural frequencies due to the sag, and the in-plane direct excitation term $\hat{X}_{zn}$ includes a contribution from axial end motion (again for odd modes only, due to the sag), in contrast to that for out-of plane direct excitation, $\hat{X}_{yn}$.

In Section 3 the above equations are manipulated algebraically to give the steady state modal amplitudes in different combinations of modes, in terms of the roots of polynomials. The stability of the solutions is addressed in Section 4 and validation of the results is covered in Section 5.

2.3. Assumptions

Before presenting the analytical solutions it is appropriate to note the assumptions underlying the analysis herein. The analysis is based on the cable model from Warnitchai et al. [34], which has its limitations, as does any model. Its main assumptions are that:

(i) The axial wave propagation speed ($=\sqrt{(E/\rho)}$) is much higher than the transverse wave propagation speed ($=\sqrt{(\sigma_s/\rho)}$), leading to the condition that $\sqrt{\varepsilon_s} \ll 1$. This condition is met for materials with a high Young's modulus, such as steel.

(ii) The static angular deviation of the cable orientation from the chord orientation (α_s) is small, such that $\tan\alpha_s \approx \alpha_s$. Regarding the static sag this is commonly considered to be satisfied if the mid-span sag normal to the chord is less than $L/8$, which is equivalent to the condition $\Gamma\cos\theta < 1$ and is commonly called a 'low sag' cable. It is then also generally considered that the parabolic sag profile is a reasonable approximation to the actual profile. For stay cables, such as on cable-stayed bridges, normally $\Gamma\cos\theta < 0.1$, that is to say that the mid-span sag normal to the chord is of the order of 1% of the length or less, so this assumption is well satisfied.

(iii) Similarly, the dynamic angular deviation of the cable orientation (α_d) from the static configuration is small, such that $\tan(\alpha_s+\alpha_d) \approx (\alpha_s+\alpha_d)$. This means that the non-dimensional modal displacement amplitudes, $\tilde{y}_{nc}$, $\tilde{y}_{ns}$, $\tilde{z}_{nc}$ and $\tilde{z}_{ns}$, are small ($\ll 1$), implying that the non-dimensional input amplitudes, $\hat{X}_{yn}$, $\hat{X}_{zn}$ and $\hat{U}$, are small ($\ll 1$). This latter point is also behind the assumption that the strictly nonlinear relationship between tension and axial strain, due to the sag effect, can be linearised using Ernst's equivalent modulus, E_q. In practice these conditions are met for bridge stay cables, although for cables hundreds of metres long the physical response amplitudes may still be many metres.

(iv) The detuning of the in-plane modes from the natural frequencies of a taut string is small ($\kappa_n \ll 1$) and the mode shapes are close to the pure sine mode shapes of a taut string. This occurs when $\lambda^2 \leq \mathrm{O}(1)$. This is normally satisfied for stay cables, for which the detuning is of the order of a few percent or less.

In the scaling and averaging analysis it is further assumed that:

(v) The damping ratios of all modes, ξ_{zn} and ξ_{yn}, are small. Even with added dampers, for stay cables these values are typically less than 1%.

(vi) The excitation frequency is close to one of the natural frequencies of the cable, i.e. $|\mu| \ll 1$. These are of course frequency ranges where large responses are expected. As the magnitude of the detuning becomes greater the accuracy of the approximation used is expected to decrease.

(vii) Each mode responds only near its natural frequency. This assumption is revisited in Section 5.

As argued under each of the above assumptions, they are reasonable for taut cables such as on cable stayed bridges. The most restrictive condition is the normally the one on λ^2 given by assumption (iv). As cables become longer or have lower tension this assumption becomes more questionable, but even for one of the longest cables on the Pont de Normandie, at 440 m long (Stay 1 in [22]), $\lambda^2 = 1.77$ and $\kappa_1 = 0.07$, so the assumption is reasonable. In relation to assumption (i), for this

cable $\sqrt{\varepsilon_s}=0.05$ and in relation to (ii), $\Gamma\cos\theta=0.07$ and the mid-span sag normal to the chord is 0.9% of the length, so these other assumptions are also satisfied.

For cables with greater sag, such as suspension cables or electricity transmission lines, assumption (iv) is not generally valid, even if assumption (ii) holds so the cable may otherwise be considered as 'low sag'. For such cables there has been much other research, particularly regarding modal interactions in the crossover regions e.g. [6–9], the first of which occurs when the first in-plane natural frequency equals the second in-plane and out-of-plane natural frequency, when $\lambda^2=4\pi^2$.

3. Solutions for steady state amplitudes in different combinations of modes

Having derived Eqs. (7)–(10) in Section 2.2, which must be satisfied for all modes for steady state solutions, they are manipulated here to obtain polynomial expressions, the roots of which give the amplitudes of steady state vibrations in various combinations of modes. Thus, apart from finding the roots of one polynomial for each solution, the steady state amplitudes can be found without recourse to numerical methods.

In Eqs. (7)-(10), an axial end input $\hat{U}$ potentially parametrically excites both the in-plane and out-of-plane modes close to half the excitation frequency ($p=2n$). $\hat{X}_{yn}$ directly excites the out-of-plane mode at the excitation frequency ($p=n$) and similarly $\hat{X}_{zn}$the equivalent in-plane mode. Nonlinear coupling could excite other modes. Inclined cables often experience in-plane motion of the ends providing combined $\hat{U}$ and $\hat{X}_{zn}$ inputs. Out-of-plane inputs give similar behaviour to $\hat{X}_{zn}$ inputs but without the $\hat{U}$ component. External forcing on the cable, F_{yn} and F_{zn}, is allowed for in $\hat{X}_{yn}$ and $\hat{X}_{zn}$ (Eq. (11c and d)) but it does not provide parametric excitation. To cover the more general case of combined inputs, hereafter in this paper, except where stated otherwise, in-plane support inputs are considered, in the form of vertical motion of the lower end (δ in Fig. 1) of non-dimensional amplitude $\hat{\Delta}$, so $\hat{U}=\hat{\Delta}\ \sin\ \theta$, $\hat{W}_n=(-1)^{n+1}\hat{\Delta}\ \cos\ \theta$ and $\hat{V}_n=F_{yn}=F_{zn}=0$ (hence $\hat{X}_{yn}=0$ and $\hat{X}_{zn}$ is given by Eq. (11d)). The responses for out-of-plane support inputs and external direct excitation are not explicitly derived but they are equivalent to simplified cases of the solutions provided.

Firstly, the response of modes that are not directly or parametrically excited is considered. For $2n\neq p$ (i.e. for any modes other than the one in each plane potentially excited parametrically), Eq. (8) $\times\,\tilde{z}_{ns}$–Eq. (7) $\times\,\tilde{z}_{nc}$ gives

$$-\xi_{yn}\tilde{C}_n+b_{yn}\tilde{D}_n=-\delta_{n,p}\hat{X}_{yn}\tilde{z}_{ns} \tag{12}$$

where $\tilde{D}_n=\tilde{y}_{nc}\tilde{z}_{ns}-\tilde{y}_{ns}\tilde{z}_{nc}$.

Similarly, Eq. (7) $\times\,\tilde{y}_{ns}$+Eq. (8) $\times\,\tilde{y}_{nc}$ gives

$$b_{yn}\tilde{Y}_n^2-\frac{1}{16\varepsilon_s}\tilde{C}_n^2=-\delta_{n,p}\hat{X}_{yn}\tilde{y}_{nc}, \tag{13}$$

and Eq. (9) $\times\,\tilde{z}_{nc}$–Eq. (10) $\times\,\tilde{z}_{ns}$ gives

$$\xi_{zn}\tilde{Z}_n^2+\frac{1}{16\varepsilon_s}\tilde{C}_n\tilde{D}_n=\delta_{n,p}\hat{X}_{zn}\tilde{z}_{ns}. \tag{14}$$

Also, for later reference, Eq. (9) $\times\,\tilde{z}_{ns}+$ Eq. (10) $\times\,\tilde{z}_{nc}$ gives

$$b_{zn}\tilde{Z}_n^2-\frac{1}{16\varepsilon_s}\tilde{C}_n^2=-\delta_{n,p}\hat{X}_{zn}\tilde{z}_{nc} \tag{15}$$

Table 1
Parameter values for a typical mid-length bridge stay-cable.

Basic parameters from Ben-Ahin Bridge cable [22]:	Length, L	110.5 m
	Cross-sectional area, A	8260 mm^2
	Mass per unit length, ρA	64.84 kg m^{-1}
	Young's modulus, E	210×10^9 N m^{-2}
	Static tension, $\sigma_s A$	4895 kN
Additional assumed parameters:	Inclination angle, θ	30°
	Damping ratio in all modes, ξ_{yn}, ξ_{zn}	0.3%
Non-dimensional parameters:	Static strain, $\varepsilon_s=\sigma_s/E$	2.82×10^{-3}
	Ratio of cable weight to tension, $\Gamma=\rho gL/\sigma_s$	0.0144
	Irvine's parameter, $\lambda^2=\Gamma^2\cos^2\theta/\varepsilon_s$	0.0548
	1st in-plane mode detuning, $\kappa_1=4\lambda^2/\pi^4$	2.25×10^{-3}
	3rd in-plane mode detuning, $\kappa_3=4\lambda^2/81\pi^4$	0.0278×10^{-3}
Natural frequencies:	1st out-of-plane, $\omega_{y1}/2\pi$	1.243 Hz
	1st in-plane, $\omega_{z1}/2\pi$	1.246 Hz
	2nd out-of-plane and in-plane, $\omega_{y2}/2\pi$, $\omega_{z2}/2\pi$	2.486 Hz
	3rd out-of-plane and in-plane, $\omega_{y3}/2\pi$, $\omega_{z3}/2\pi$	3.730 Hz

and Eq. (7) $\times \tilde{z}_{ns}$ + Eq. (8) $\times \tilde{z}_{nc}$ gives

$$\xi_{yn}\tilde{D}_n + b_{yn}\tilde{C}_n - \frac{1}{16\varepsilon_s}\tilde{C}_n\tilde{Z}_n^2 = -\delta_{n,p}\hat{X}_{yn}\tilde{z}_{nc}. \tag{16}$$

For $n \neq p$ (and $2n \neq p$), eliminating $\tilde{C}_n$ and $\tilde{D}_n$ from Eqs. (12)–(14) yields

$$\xi_{yn}\tilde{Y}_n^2 + \xi_{zn}\tilde{Z}_n^2 = 0. \tag{17}$$

Hence, based on the averaged modulation equations Eqs. (3)–(6), for positive damping there are no non-zero real solutions for $\tilde{Y}_n$ and $\tilde{Z}_n$, hence non-zero steady state responses can only exist for $n=p$ or $n=p/2=q$, i.e. for the modes at the excitation frequency and at half this frequency, namely modes y_p, z_p, y_q and z_q. This result was previously found for a taut string with equal damping in all modes [24]. Here it is found to be a more general result, for cables with small sag and for different (but always positive) damping in each mode. Based on this result, hereafter where b_{yn} and b_{zn} (defined in Eq. (11)) are used it is only necessary to sum over p and q rather than over all modes. It should be noted that the modal interactions considered here, for a taut cable close to 2:2:1:1 internal resonance, are different from those previously addressed for slacker cables around frequency crossovers [6–9], which are close to 2:2:2:1 internal resonance.

Strictly other responses can occur, which are lost in the averaging analysis. The averaging assumes that each mode only responds close to its natural frequency, but in reality all modes (in the relevant plane) can respond to a small degree at the excitation frequency. One special case where this can become significant and can lead to noticeable responses at twice the excitation frequency has been identified [32]. However, the conditions for that behaviour are unusual and it is believed that it is normally adequate to use the averaged equations, as discussed by Bajaj and Johnson [15] and as applied throughout this paper.

In the following sub-sections, different steady state solutions are considered, involving different combinations of modes. Example results are shown using parameter values for a typical mid-length bridge stay-cable, given in Table 1. The basic parameters are from a cable on the Ben-Ahin Bridge [22]. The reference does not give the inclination angle for the specific cable so a typical value of 30° is used. The damping ratios of bridge cables without external dampers are normally below 0.5% see e.g. [37]. Here a value of 0.3% is used for all modes, which enables the key features in the response plots to be identified. Table 1 also shows the non-dimensional parameters and natural frequencies of the cable. It should be noted that the detuning of the first in-plane mode from the corresponding out-of plane mode (κ_1) is small and that of higher in-plane modes is negligible. This is typical for mid-length bridge cables. For long bridge cables the detuning of the first in-plane mode may be up to about 10%.

3.1. Response in directly excited mode only (z_p, solution I)

For excitation near the natural frequency of any mode, that mode, in the plane of the excitation, is always excited directly (except for purely axial input to even modes or vertical cables). For excitation in-plane with zero response in all other modes, the response amplitude in the directly excited mode can be found from Eq. $(9)^2$ + Eq. $(10)^2$ with $n=p$, yielding

$$\frac{9}{(32\varepsilon_s)^2}\tilde{Z}_p^6 - \frac{6}{32\varepsilon_s}(\mu-\kappa_p)\tilde{Z}_p^4 + \left((\mu-\kappa_p)^2+\xi_{zp}^2\right)\tilde{Z}_p^2 = \hat{X}_{zp}^2. \tag{18}$$

This expression is as found previously [32]. It is a cubic equation in the non-dimensional response amplitude squared, $\tilde{Z}_p^2$. For $\kappa_p=0$ it is equivalent to an expression given by Nayfeh and Mook for a taut string [13] and for a cable with small sag, for which $\kappa_p \neq 0$ and the excitation $\hat{X}_{zp}$ is affected by the sag (Eq. (11d)), it has been shown to match experimental results well [35]. The maximum response is given by $\tilde{Z}_p = \hat{X}_{zp}/\xi_{zp}$, which is the same as for the linear system (i.e. Eq. (2) but ignoring all nonlinear terms), but it occurs at $\mu = \frac{3}{32\varepsilon_s}\tilde{Z}_p^2 + \kappa_p$, rather than at $\mu = \kappa_p$ for the linear system, because of the increase in mean tension due to the nonlinearity.

Eq. (18) gives the response that occurs when all other modes are stable about zero amplitude, which generally occurs when the amplitude of the input is below some threshold value, which is frequency dependent. The stability boundaries of this solution, beyond which other modes are excited and the response in mode z_p is modified, were covered in the previous paper [32]. The following sub-sections give the steady state responses in two or three modes beyond the stability boundaries of the above solution.

3.2. Response in directly excited mode (z_p) and corresponding mode in the other plane (y_p) through nonlinear coupling (solution II)

For a cable with low sag the modes are in pairs – one mode in each plane – with close natural frequencies. For even modes (or no sag, e.g. taut strings or vertical cables) the natural frequencies are the same in the two planes but for odd modes there is small detuning, κ_n, due to the sag.

In certain conditions the nonlinear modal coupling can cause excitation of the paired mode in the plane not excited directly, as well as in the directly excited mode. The resulting non-planar behaviour has previously been addressed for taut

strings with equal damping in both planes [13–15]. It is considered here for the more general case of a cable with low sag, hence detuning, and different damping in the two planes.

For $n=p$ and excitation in-plane $\left(\hat{X}_{yp}=0\right)$, taking Eq. (14)^2+Eq. (15)^2 and substituting for $\tilde{D}_n/\tilde{C}_n$ and $\tilde{C}_n^2$ from Eqs. (12) and (13) respectively leads to

$$\left(\xi_{yp}\tilde{Y}_p^2+\xi_{zp}\tilde{Z}_p^2\right)^2+\left(b_{yp}\tilde{Y}_p^2-b_{zp}\tilde{Z}_p^2\right)^2=\hat{X}_{zp}^2\tilde{Z}_p^2. \tag{19}$$

Also substituting for $\tilde{D}_n/\tilde{C}_n$ in Eq. (16) gives

$$\xi_{yp}^2+b_{yp}\left(b_{yp}-\frac{1}{16\varepsilon_s}\tilde{Z}_p^2\right)=0 \tag{20}$$

or $\tilde{C}_p=0$.

Eqs. (19) and (20) are two nonlinear equations in $\tilde{Y}_p$ and $\tilde{Z}_p$ (and in general $\tilde{Y}_q$ and $\tilde{Z}_q$, see Section 3.4). For zero response in all modes except mode z_p, $\tilde{C}_p=0$ so Eq. (20) does not need to be satisfied and Eq. (19) reduces to Eq. (18).

Putting $\tilde{Y}_p=0$ (and zero response in all other modes except z_p) in Eq. (20) gives

$$\frac{3}{(32\varepsilon_s)^2}\tilde{Z}_p^4-\frac{4}{32\varepsilon_s}\mu\tilde{Z}_p^2+(\mu^2+\xi_{yp}^2)=0. \tag{21}$$

This corresponds to the bifurcation point beyond which non-zero responses occur in mode y_p, as found in the previous paper [32] by considering the stability of mode y_p in the presence of a non-zero response of mode z_p (and no other modal responses).

For non-zero responses in both modes y_p and z_p (but zero responses in all other modes), Eqs. (19) and (20) must both be satisfied.

Eq. (20) can be rearranged to give

$$\frac{1}{16\varepsilon_s}\tilde{Z}_p^2=-\frac{(\xi_{yp}^2+\phi^2)}{\phi} \tag{22}$$

where $\phi=\mu-\frac{3}{32\varepsilon_s}(\tilde{Y}_p^2+\tilde{Z}_p^2)$,

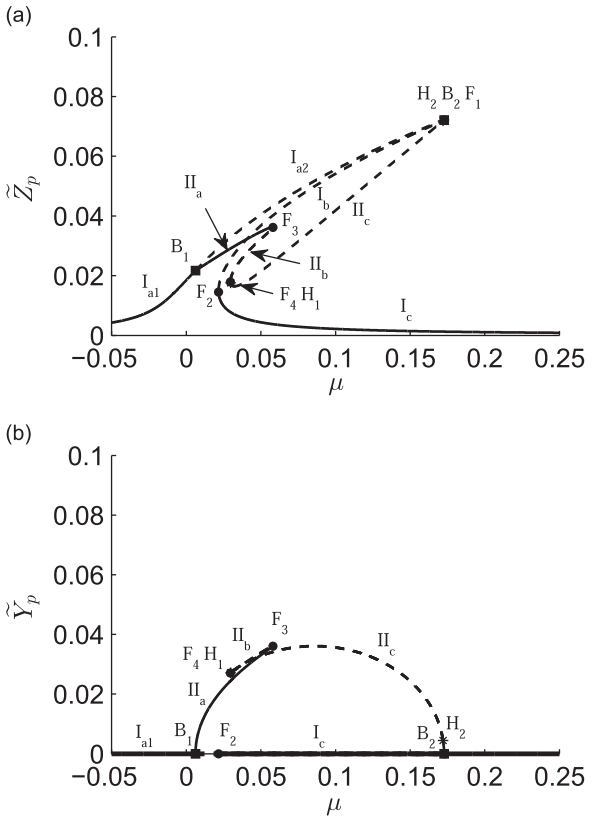

Fig. 2. Frequency response curves of modes z_p (a) and y_p (b) for the cable in Table 1 for excitation with $p=3$ for input amplitude $\hat{\Delta}=0.25\times10^{-3}$, but only including the component of the input motion normal to the cable. Solid curves, stable branches; dotted curves, unstable branches; ■, bifurcation; ●, fold; *, Hopf bifurcation.

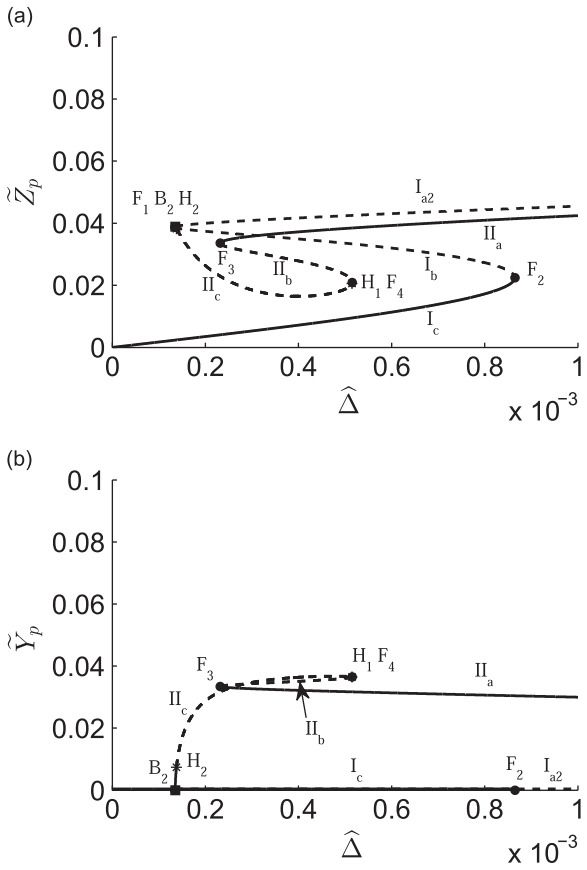

Fig. 3. Responses in modes z_p (a) and y_p (b) vs. input amplitude (only including the component normal to the cable) for the cable in Table 1 for excitation with $p=3$ for input frequency detuning $\mu=0.05$. Symbols as for Fig. 2.

hence Eq. (19) can be expressed as

$$\left\{\xi_{yp}(\mu-\phi)\phi+\frac{3(\xi_{yp}-\xi_{zp})}{2}(\xi_{yp}^2+\phi^2)\right\}^2+\left\{(3\xi_{yp}^2+\mu\phi+2\phi^2)\phi-\frac{3\kappa_p}{2}(\xi_{yp}^2+\phi^2)\right\}^2=-\frac{9\hat{X}_{zp}^2}{64\varepsilon_s}(\xi_{yp}^2+\phi^2)\phi. \tag{23}$$

This is a 6th order polynomial in ϕ. The roots give the general solutions for steady state coupled motion in the two planes for planar input (in-plane).

For perfect tuning ($\kappa_p=0$) or the same damping in the two planes ($\xi_{yp}=\xi_{zp}$), clearly the above equation simplifies. For zero damping in both planes it simplifies to the cubic expression

$$(4\phi+2\mu-3\kappa_p)^2\phi=-\frac{9\hat{X}_{zp}^2}{16\varepsilon_s}. \tag{24}$$

In any case, having solved for ϕ, from Eq. (22) and the definition of ϕ the modal amplitudes are given by

$$\widetilde{Z}_p=\sqrt{-\frac{16\varepsilon_s}{\phi}\left(\xi_{yp}^2+\phi^2\right)}, \tag{25}$$

$$\widetilde{Y}_p=\sqrt{\frac{16\varepsilon_s}{3\phi}\left(3\xi_{yp}^2+2\mu\phi+\phi^2\right)}. \tag{26}$$

Having found the modal amplitudes, the sine and cosine components, and hence the motion time histories and trajectories can be found from Eqs. (9)–(15). The signs of the y_p components can be positive or negative, indicating two solutions that are symmetrical with each other about the vertical plane.

Plots of the non-dimensional response amplitudes $\tilde{Z}_p$ and $\tilde{Y}_p$ are given in Figs. 2 and 3 for the cable in Table 1 for excitation around the 3rd mode pair ($p=3$). Excitation in this frequency range is chosen since, with odd p, there is no parametric excitation of a mode with half the natural frequency (covered in Sections 3.3 and 3.4) and the modes in the two planes are almost perfectly tuned ($\kappa_3=0.0278\times10^{-3}$, Table 1), so the system behaves effectively as a taut string. Only the

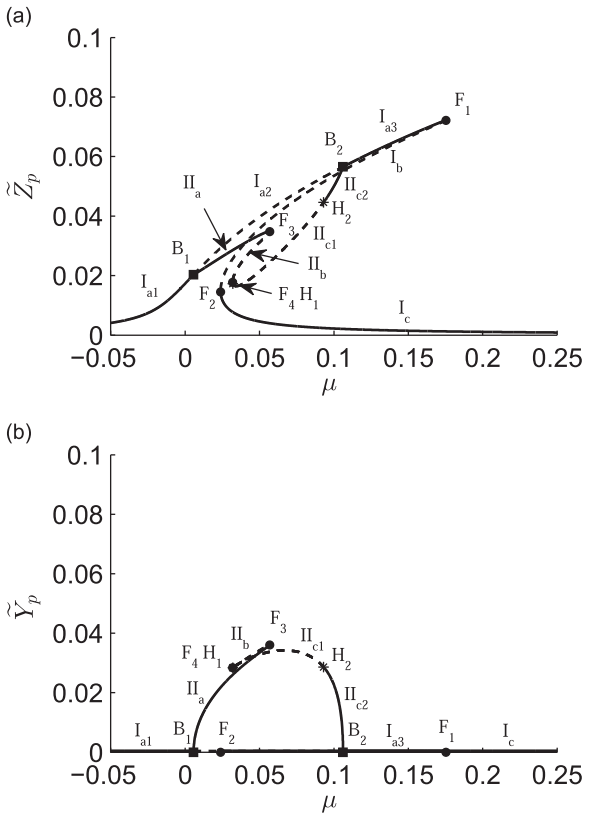

Fig. 4. Frequency response curves of modes z_p (a) and y_p (b) for the cable in Table 1 for excitation with $p=1$ for input amplitude $\hat{\Delta}=0.25\times10^{-3}$, but only including the component of the input motion normal to the cable. Symbols as for Fig. 2.

component of input motion normal to the cable is included ($\hat{W}_3=\hat{\Delta}\cos\theta$), although the only effect of the axial component would be a 5.7% reduction in the effective excitation amplitude from Eq. (11d).

Fig. 2(a) shows the $\tilde{Z}_p$ frequency response curves for a given input amplitude of $\hat{\Delta}=0.25\times10^{-3}$. The planar ($z_p$ only) response, given by Eq. (18) and designated solution I, shows a resonance curve with hardening behaviour. The lower branch, I_c, which exists for excitation frequencies above fold F_2, is stable; the middle branch, I_b, which exists between folds F_1 and F_2 is unstable, and the upper branch, which exists for excitation frequencies below fold F_1 is stable for low excitation frequencies (I_{a1}) and then becomes unstable (I_{a2}) at bifurcation point B_1, given by Eq. (21). Beyond B_1 the non-planar (z_py_p) response exists, which is given by Eqs. (23), (25) and (26) and is designated II. Branch II_a is stable and exists between B_1 and fold F_3. The response in mode y_p, shown in Fig. 2(b), causes an increase in mean cable tension which shifts the resonance curve for mode z_p towards higher frequency than for branch I_{a2}. The response in mode y_p grows from zero amplitude at B_1 to the same amplitude as mode z_p at F_3. Between F_3 and F_4 there is an unstable branch, II_b. Branch II_c links F_4 with bifurcation point B_2, given by the second solution of Eq. (21), at which the y_p response reduces to zero (Fig. 2(b)) and the non-planar branch re-joins the planar branch, very close to F_1 (Fig. 2(a)). Very close to F_4 and B_2 there are Hopf bifurcations (H_1 and H_2) on branch II_c, between which the constant amplitude solutions considered here are unstable. In this region quasi-periodic and chaotic responses can occur, as discussed in detail by Bajaj and Johnson [15].

Fig. 3 shows the cable response amplitudes in the same conditions except for varying excitation amplitude and a constant input frequency with $\mu=0.05$. Figs. 2 and 3 thus show perpendicular sections through the response amplitude surfaces in $\mu-\hat{\Delta}-\tilde{Z}_p$ and $\mu-\hat{\Delta}-\tilde{Y}_p$ spaces. The points and branches in Fig. 3 have the same labelling as the equivalent points and branches in Fig. 2, although they are at different specific values of μ and $\hat{\Delta}$. Increasing the excitation amplitude from zero the response follows the stable lower planar branch I_c up to F_2, at which there is jump up to the stable non-planar branch II_a (the upper planar branch I_{a2} being unstable). Then decreasing the excitation amplitude the response follows that branch down to F_3 at which there is a jump back down to the planar response on branch I_c or possibly to a quasi-periodic or chaotic response associated with branch II_c, which is between the two Hopf bifurcation points.

The responses in Figs. 2 and 3 are similar to those for a taut string with planar transverse end excitation presented by Nayfeh and Mook [13], who described the jumps for increasing and decreasing frequency or excitation amplitude, and by Miles [14] and Bajaj and Johnson [15], who covered the Hopf bifurcations and resulting quasi-periodic and chaotic solutions extensively.

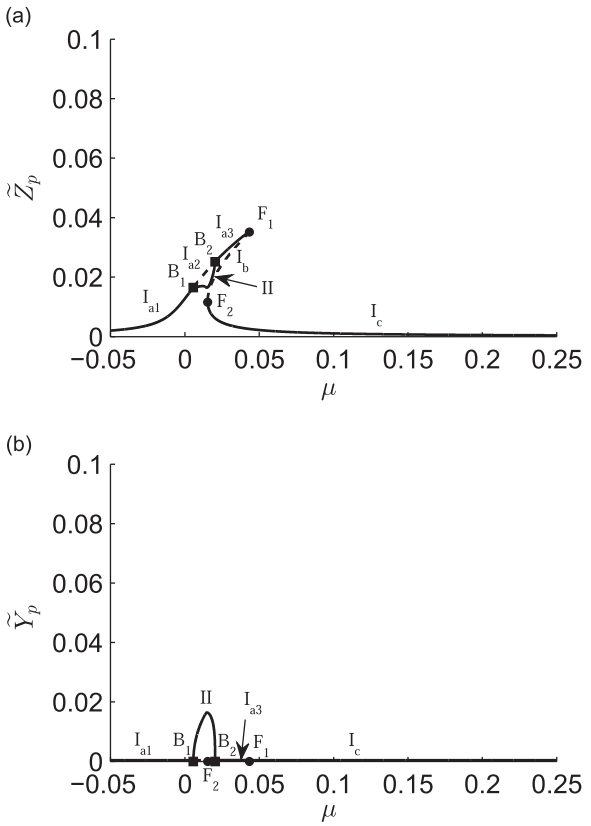

Fig. 5. Frequency response curves of modes z_p (a) and y_p (b) for the cable in Table 1 for excitation with $p=1$ for input amplitude $\hat{\Delta}=0.25\times10^{-3}$, including the components of the input motion both normal and axial to the cable. Symbols as for Fig. 2.

Going beyond previous results, the solutions here also allow for detuning of the modes in the two planes due to sag, for different damping in each mode and for the axial component of the excitation. Fig. 4 shows the normalised frequency responses curves equivalent to Fig. 2 but for excitation around $p=1$ rather than $p=3$. Taking the damping in all modes to be the same, the only difference in the normalised equations is the detuning between the relevant modes ($\kappa_1=2.25\times10^{-3}$, Table 1). Although the detuning is still less than 1% it makes a significant difference to the responses. In comparison with the near perfectly tuned case (Fig. 2), B_2 has moved down the upper planar (I_a) branch and H_2 has moved down non-planar branch II_c. Hence the top of the upper planar branch is stabilised (I_{a3}) and the top section of the non-planar branch is also stable (II_{c2}). There is therefore a greater range of inputs for which large steady state responses can occur than without detuning, although certain initial conditions are required to reach these solutions.

For larger detuning B_2 and B_1 eventually meet, making the whole of the upper planar branch (I_a) stable and isolating the non-planar (II) solution branches. An advantage of the proposed solutions over previous approaches using numerical continuation is that the resulting isola is found directly.

The effect of damping is to decrease the peak responses of both solutions. The maximum response of the planar solution (by F_1) is inversely proportional to the damping in mode z_p, as described in Section 3.1. For $\kappa_p=0$ the sum of the damping in modes y_p and z_p appears to govern the peak non-planar response amplitude (by F_3). When modes y_p and z_p are detuned the damping in mode y_p has a greater effect on the non-planar response than the damping in mode z_p.

Fig. 5 shows the frequency response curves of modes z_p and y_p for $p=1$ for the same conditions as Fig. 4, except with the axial component of the end input motion now also included. Since p is odd there is still no parametric excitation but there is a 51% reduction in the effective excitation amplitude, $\hat{X}_{zp}$, due to the axial component of the input, $\hat{U}$ (see Eq. (11d)), which causes dynamic variation in the sag thus giving direct excitation of odd modes, particularly the first. This effect is often overlooked in the analysis of bridge cable vibrations due to support motions but its significance has recently been highlighted [35], whilst direct excitation of the first in-plane mode was previously considered in the context of a cable in the first crossover region [6]. Fig. 5 shows that the maximum responses in both the planar and non-planar solutions are reduced. Also in this instance the whole of the non-planar branch is now stable, as well as the top of the upper planar branch.

3.3. Response in directly excited mode (z_p) and parametrically excited mode in either plane (y_q, solution III, or z_q, solution IV)

Based on the averaged equations to first order ε, parametrically excited responses only occur when the excitation is close to two times a natural frequency ($p=2n$) and there is an end motion input with a component longitudinal to the cable ($\hat{U}\neq 0$) (see Eqs. (7)–(10)). Pure out-of-plane excitation does not contain a component along the cable axis so does not give parametric excitation, so response to excitation in this plane is only ever in mode y_p only or in modes y_p and z_p, as covered in the previous two sub-sections. In-plane excitation often includes components both transverse and axial to the cable. There is then a response in the directly excited mode (z_p) and potentially in a parametrically excited mode (z_q or y_q, where $q=p/2$). The nonlinear coupling means that these two responses affect each other. This sub-section considers the case of the response in modes z_p and z_q only (parametric response of mode y_q is similar). The next sub-section includes a response in mode y_p also.

Considering the directly excited mode ($n=p$, with even p so mode q exists), from Eq. (19) with $\tilde{Y}_p=0$,

$$\tilde{Z}_p^2(\xi_{zp}^2+b_{zp}^2)=\hat{X}_{zp}^2 \tag{27}$$

(or $\tilde{Z}_p=0$, but this would not apply when there is direct excitation of mode z_p).

Note that since p is even, $\kappa_p=0$, the $\hat{U}$ term in $\hat{X}_{zp}$ is zero, and for no external force on the cable $\hat{X}_{zp}=\hat{W}_p$. Further note that b_{zp} now includes a contribution from mode z_q (or y_q), rather than y_p, as in the previous sub-section. For $\tilde{Z}_q=0$, Eq. (27) agrees with the previous expression for the steady state amplitude of the directly excited mode alone, Eq. (18).

Considering the parametrically excited mode, Eq. (9)^2+Eq. (10)^2, with $n=q=p/2$ and a response in mode z_q (but not y_q, hence $\tilde{C}_q=0$), leads to

$$\xi_{zq}^2+{b_{zq}}^2=\left(\frac{\hat{U}}{4\varepsilon_s(1+\lambda^2/12)}\right)^2 \tag{28}$$

or $\tilde{Z}_q=0$, i.e. no parametrically excited response.

Putting $\tilde{Z}_q=0$ (and zero response in all other modes except z_p) in Eq. (28) gives

$$\frac{4}{(32\varepsilon_s)^2}\tilde{Z}_p^4-\frac{4}{32\varepsilon_s}(\mu-\kappa_q)\tilde{Z}_p^2+(\mu-\kappa_q)^2+\xi_{zq}^2=\left(\frac{\hat{U}}{4\varepsilon_s(1+\lambda^2/12)}\right)^2. \tag{29}$$

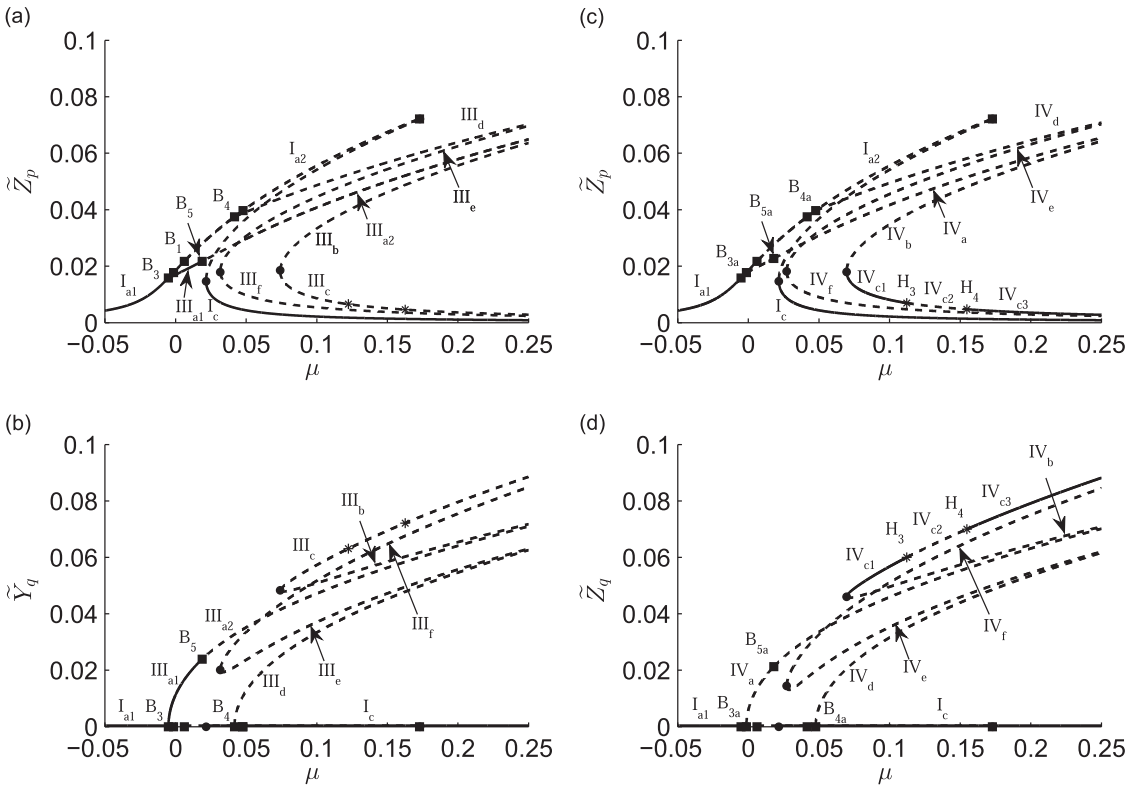

Fig. 6. Frequency response curves of modes z_p (a and c), y_q (b) and z_q (d) for the cable in Table 1 for excitation with $p=2$ for input amplitude $\hat{\Delta}=0.25\times 10^{-3}$. (a) and (b) show solutions I and III whilst (c) and (d) show solutions I and IV. Symbols as for Fig. 2.

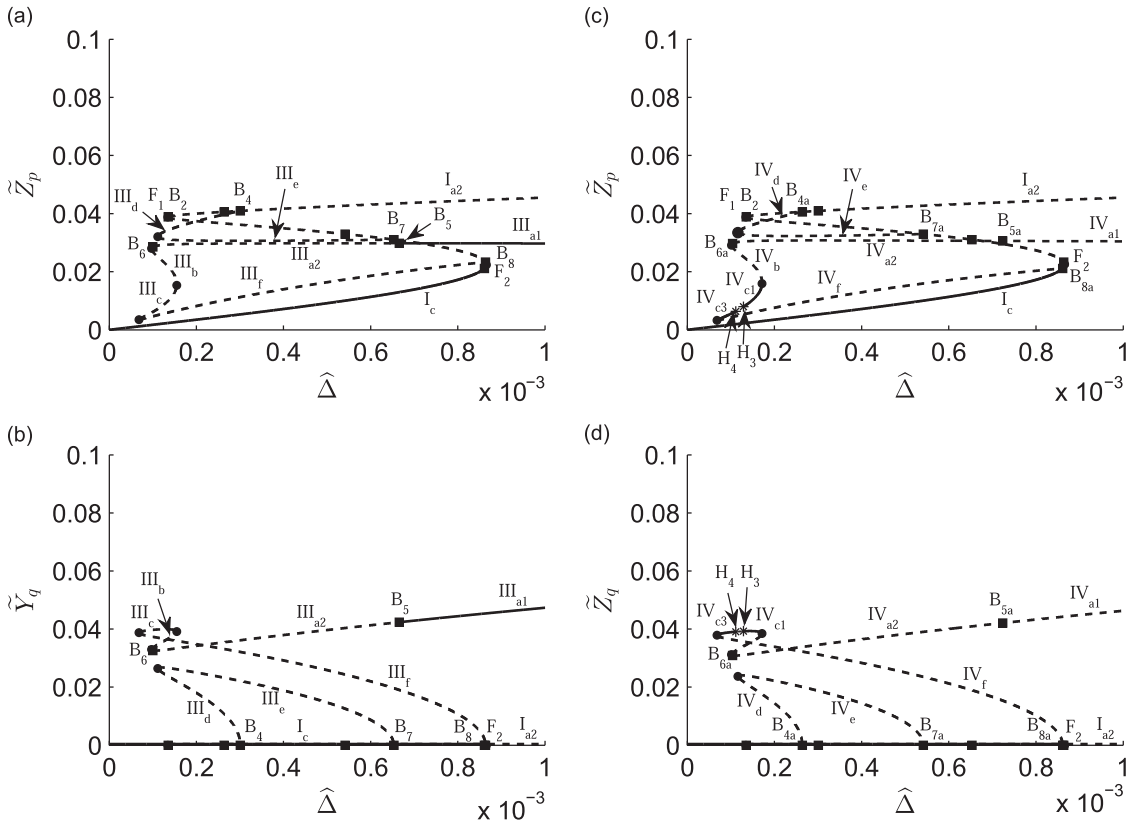

Fig. 7. Responses in modes z_p (a and c), y_p (b) and z_q (d) vs. vertical input amplitude for the cable in Table 1 for excitation with $p=2$ for input frequency detuning $\mu=0.05$. (a) and (b) show solutions I and III whilst (c) and (d) show solutions I and IV. Symbols as for Fig. 2.

This defines the stability boundary beyond which parametric response occurs in mode z_q, as previously found by considering the stability of mode z_q (or y_q) in the presence of a directly excited response of mode z_p [32]. It has been found to match experimental results well, for both in-plane and out-of-plane modes [32,35]. Setting $\tilde{Z}_p = 0$, Eq. (29) agrees, to first order ε, with equations for the stability boundary for parametric responses from previous authors [10,22], except the current equation allows for the effects of sag, which causes $\hat{U}$ to be reduced by a factor of $(1+\lambda^2/12)$ and, for odd in-plane modes, detuning of the natural frequency. A response in mode z_p, which is always non-zero when there is a component of excitation transverse to the cable, clearly modifies the stability boundary.

Eqs. (27) and (28) together define the simultaneous steady state responses in the directly excited and parametrically excited modes.

By expanding b_{zq}, with responses only in modes z_p and z_q, Eq. (28) can be rearranged to give

$$\tilde{Z}_q^2 = \frac{32\varepsilon_s}{3}\{\mu - \kappa_q - S\} - \frac{2}{3}\tilde{Z}_p^2 \tag{30}$$

where $S = \pm\sqrt{\left(\frac{\hat{U}}{4\varepsilon_s(1+\lambda^2/12)}\right)^2 - \xi_{zq}^2}$.

Hence, when mode z_q is parametrically excited, substituting Eq. (30) in b_{zp} in Eq. (27), the response amplitude in mode z_p is given by

$$\tilde{Z}_p^2\left[9\xi_{zp}^2 + \left\{\mu + 2\kappa_q - \frac{5}{32\varepsilon_s}\tilde{Z}_p^2 + 2S\right\}^2\right] = 9\hat{X}_{zp}^2 \tag{31}$$

This is a cubic equation in $\tilde{Z}_p^2$. There are 6 roots since S can be positive or negative. Having solved Eq. (31) for $\tilde{Z}_p$, $\tilde{Z}_q$ is given by Eq. (30).

There is an identical pair of equations for parametric response in mode y_q rather than z_q, but without κ_q and with S defined using ξ_{yq} rather than ξ_{zq}.

Ignoring the response in the directly excited mode, $\tilde{Z}_p$, Eq. (30) is the same, to first order ε, as equations from previous authors [10,11,20,25] for the parametrically excited response amplitude of the first mode, except the current equation allows for any mode and for the effects of sag. The effect of the response in the directly excited mode is to reduce the amplitude of

the parametrically excited mode. However, since the stability boundary is also affected, as described above, parametrically excited vibrations may occur for some inputs in the presence of mode z_p that would not occur without it.

Fig. 6 shows the frequency response curves of the directly and parametrically excited modes for the cable in Table 1 for excitation around the 2nd mode pair ($p=2$) for input amplitude $\hat{\Delta} = 0.25 \times 10^{-3}$. Solution I ($z_p$ only) is the same as in Figs. 2 and 4 (except for its stability), but now, since p is even, the axial component of the input does not influence the effective direct excitation of mode p but it can cause parametric excitation of mode q in each plane. Fig. 6(a and b) shows solution III, with responses in modes z_p and y_q, whereas Fig. 6(c and d) show solution IV, with responses in modes z_p and z_q. Fig. 7 shows the same solutions plotted against the vertical input amplitude for a given input frequency. It is clear that the curves for solutions III and IV are very similar. In Fig. 6(a and c) they both show two resonance curves shifted to the right of solution I, due to the increase in mean cable tension from the response in the parametrically excited mode. The two curves represent the solutions for the alternative signs of S. For the parameter values considered, the solutions with positive S ($\mathrm{III_{d\text{-}f}}$, $\mathrm{IV_{d\text{-}f}}$) are always unstable. Since in the example the same damping was used for all modes, the differences between solutions III and IV are only due to the slight increase in the natural frequency of mode z_q due to the sag. The result is that there is a region

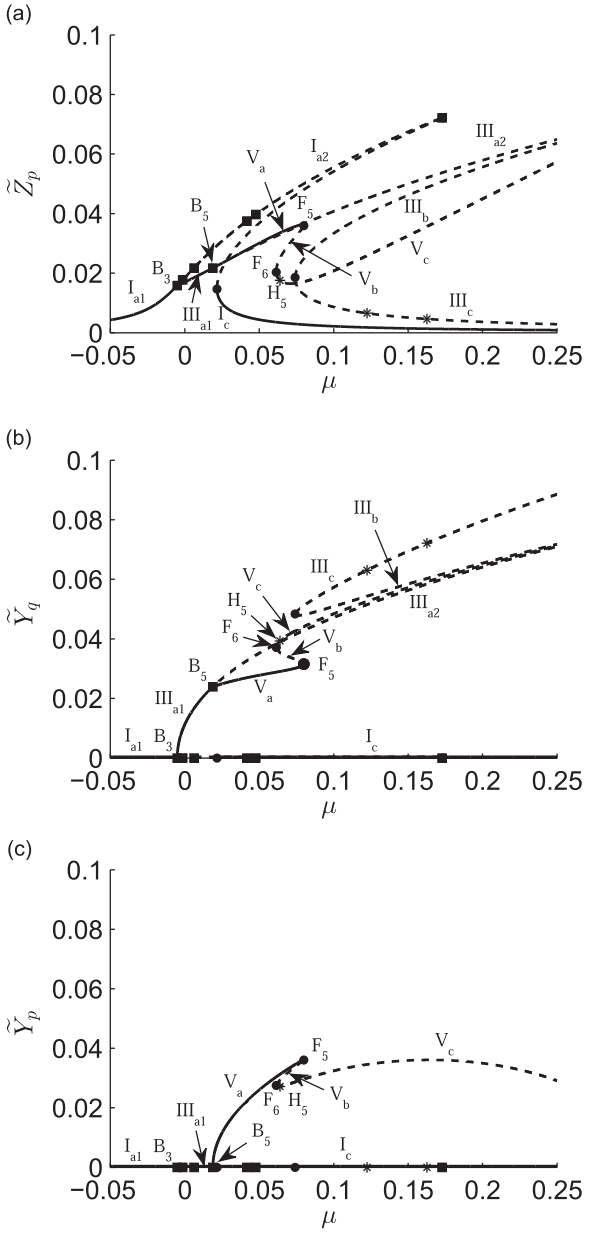

Fig. 8. Frequency response curves of modes z_p (a), y_q (b) and y_p (c) for the cable in Table 1 for excitation with $p=2$ for input amplitude $\hat{\Delta} = 0.25 \times 10^{-3}$. Only solutions with negative S are shown. Symbols as for Fig. 2.

with a stable parametrically excited response in mode y_q, along with mode z_p, around $\mu=0$ (III_{a1}, Fig. 6(a and b)) and a stable parametrically excited response in mode z_q, along with mode z_p, for higher excitation frequencies ($\mu>0.07$ for $\hat{\Delta}=0.25\times10^{-3}$, IV_c, Fig. 6(c and d)).

Branch III_a departs from branch I_a at B_3 (Fig. 6(a)), given by Eq. (29), which, for these parameter values, is below B_1, where branch II_a starts (c.f. Fig. 2(a)). Hence in this case for even p, branch II_a is unstable and for excitation around $\mu=0$ there is a stable response in modes z_p and y_q rather than in z_p and y_p. Solution II, although unstable, still exists but it is not shown on Figs. 6 and 7 for clarity. Branch III_a becomes unstable at B_5 at which there is a bifurcation to a 3-mode response (see Section 3.4). For increasing input amplitude from rest, Fig. 7(a and b) show the response follows branch I_c up to F_2 (as also in Fig. 3) at which there is a jump up to solution III_a (rather than solution II_a).

Fig. 6(c and d) show that branch IV_c is generally stable, with a moderate response in mode z_p (larger in amplitude than for the z_p only solution, I_c), accompanied by large response in mode z_q, but Fig. 7(c and d) show that this branch is not

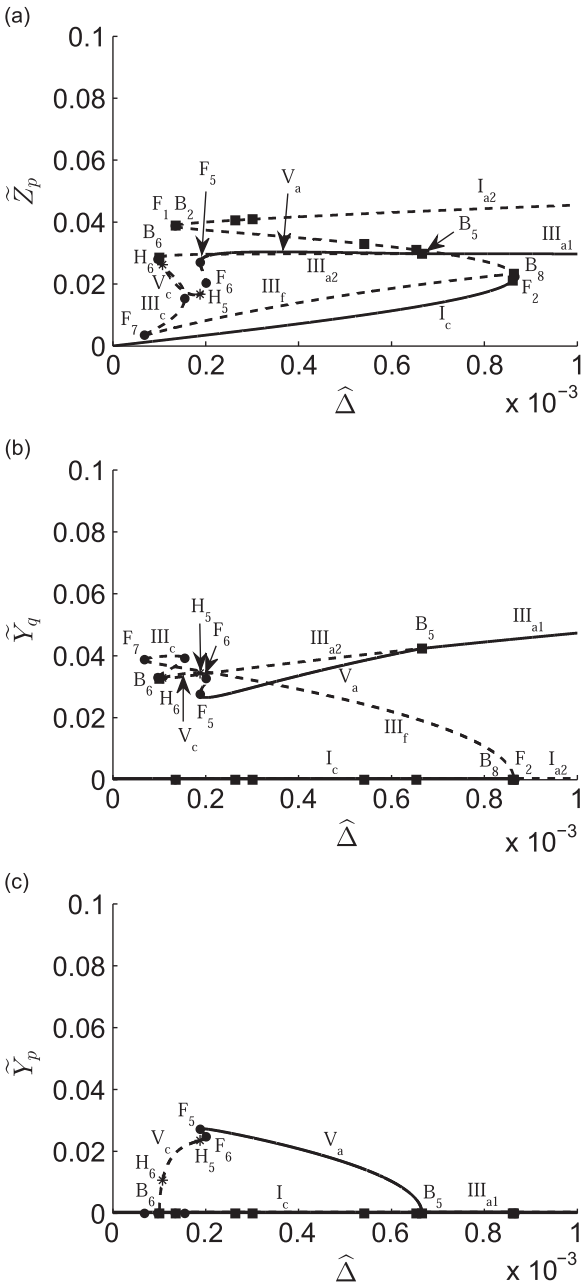

Fig. 9. Responses in modes z_p (a), y_q (b) and y_p (c) vs. vertical input amplitude for the cable in Table 1 for excitation with $p=2$ for input frequency detuning $\mu=0.05$. Only solutions with negative S (and branch III_f) are shown. Symbols as for Fig. 2.

reached increasing the input amplitude from zero. Particular initial conditions are needed to reach this branch. There are two Hopf bifurcations on the branch, H_3 and H_4, between which it is unstable. There may be quasi-periodic or chaotic solutions in this vicinity.

3.4. Response in three modes: directly excited (z_p), nonlinearly coupled in the other plane (y_p) and parametrically excited in either plane (y_q, solution V, or z_q, solution VI)

The final combination of modes to be considered is parametric excitation of mode z_q or y_q together with the directly excited mode z_p, as in the previous sub-section, but with the addition of a response in mode y_p through nonlinear coupling. As before, for there to be a parametrically excited response, there needs to be an axial component of end motion close to two times a natural frequency. The solution is derived for a response in mode z_q, since it includes κ_q. The solution for mode y_q instead is similar.

For response in three modes, Eqs. (19) and (20), for the response in modes z_p and y_p, and Eq. (28), for the parametric response in mode z_q, are still valid. However, b_{yp}, b_{zp} and b_{zq} (or b_{yq}) now need to include the contributions from all three participating modes.

By expanding b_{zq}, Eq. (28) can be rearranged to give now

$$\tilde{Z}_q^2 = \frac{32\varepsilon_s}{3}(\mu - \kappa_q - S) - \frac{2}{3}(\tilde{Y}_p^2 + \tilde{Z}_p^2). \tag{32}$$

Eq. (32) is identical to Eq. (30) except the response in mode y_p has now been included.

Expanding b_{yp} in Eq. (20) and substituting for $\tilde{Z}_q$ from Eq. (32), it can now be rearranged to give

$$\frac{1}{16\varepsilon_s}\tilde{Z}_p^2 = -\frac{(\xi_{yp}^2 + \psi^2)}{\psi} \tag{33}$$

where $\psi = \frac{1}{3}\left\{\mu + 2\kappa_q + 2S - \frac{5}{32\varepsilon_s}(\tilde{Y}_p^2 + \tilde{Z}_p^2)\right\}$,

This is different from Eq. (22) due to the inclusion of mode z_q.

Eq. (19) can now be expressed as

$$\left\{\xi_{yp}(\mu + 2\kappa_q + 2S - 3\psi)\psi + \frac{5(\xi_{yp} - \xi_{zp})}{2}(\xi_{yp}^2 + \psi^2)\right\}^2 + \left\{5(\xi_{yp}^2 + \psi^2) + (\mu + 2\kappa_q + 2S - 3\psi)\psi\right\}^2\psi^2 = -\frac{25\hat{X}_{zp}^2}{64\varepsilon_s}(\xi_{yp}^2 + \psi^2)\psi \tag{34}$$

This is a 6th order polynomial in ψ and note S can be positive or negative. The roots give the general solutions for steady state amplitudes of the three modes for planar input (in-plane).

For zero damping in all modes, Eq. (34) simplifies to

$$\left(\mu + 2\kappa_q \pm 2\frac{\hat{U}}{4\varepsilon_s(1 + \lambda^2/12)} + 2\psi\right)^2\psi = -\frac{25\hat{X}_{zp}^2}{64\varepsilon_s} \tag{35}$$

In any case, having solved for ψ, from Eqs. (32), (33) and the definition of ψ, the modal amplitudes are given by

$$\tilde{Z}_p = \sqrt{-\frac{16\varepsilon_s}{\psi}\left(\xi_{yp}^2 + \psi^2\right)} \tag{36}$$

$$\tilde{Y}_p = \sqrt{\frac{16\varepsilon_s}{5}\left(\frac{5\xi_{yp}^2}{\psi} - \psi + 2\mu + 4\kappa_q + 4S\right)} \tag{37}$$

$$\tilde{Z}_q = \sqrt{\frac{32\varepsilon_s}{5}(2\psi + \mu - 3\kappa_q - 3S)} \tag{38}$$

There is an identical set of equations for parametric response in mode y_q rather than z_q, along with z_p and y_p, but without κ_q and with S defined using ξ_{yq} rather than ξ_{zq}.

Fig. 8 shows the frequency response curves for solutions involving the three modes z_p, y_q and y_p with negative S for the cable in Table 1 with $p=2$ for a given input amplitude. The 3-mode stable solution V_a bifurcates from branch III_a at B_5. Thereafter, up to F_5, the response in mode z_p is very similar to what it is on unstable branch III_{a2} (Fig. 8(a)) but the parametrically excited response in mode y_q is reduced (Fig. 8(b)). The responses in modes z_p, and y_p (Fig. 8(a and c)) are similar to what they are on branch II_a (Fig. 2) but shifted to higher frequency due to the increased mean tension from the response in mode y_q. After F_5 the topology of solution V continues to be similar to that of solution II. There is an unstable branch, V_b, between F_5 and F_6, a Hopf bifurcation, H_5, close to F_6 and the solution rejoins solution III close to its apex just after another Hopf bifurcation. After F_6 $\tilde{Y}_q$ is similar to what it is on branch III_a.

Fig. 9 shows the steady state solutions involving the three modes z_p, y_q and y_p with negative S for variable input amplitude for a given excitation frequency. For increasing input amplitude from rest the response is initially only in mode z_p on branch I_c, then at F_2 there is a jump up to branch III_a (as also in Fig. 7). However, for a subsequent reduction in input amplitude there is a bifurcation at B_5 at which a response in mode y_p is initiated (Fig. 9(c)). As in Fig. 8, the resulting stable 3-mode solution, branch V_a, has a similar response in mode z_p to branch III_{a2} (Fig. 9(a)), but the response in mode y_q is reduced (Fig. 9(b)). As the input amplitude continues to decrease there is a jump at F_5 back down to branch I_c or possibly to a quasi-periodic or chaotic solution associated with branch II_c (Fig. 3) or V_c (Fig. 9).

The 3-mode response (solution V) with positive S bifurcates off branch II_c. It is unstable for the parameter values considered so for clarity it is not shown on Figs. 8 and 9. Solution III with positive S is also unstable so it is not shown, except for branch III_f on Fig. 9 since it joins up with III_c (at F_7 where $S=0$). As for Figs. 6 and 7, solution II is unstable so it is not shown on Figs. 8 and 9.

Solution VI, involving z_q rather than y_q, is very similar to solution V (Figs. 8 and 9) but it is unstable for the parameter values considered, except in very small regions.

No steady state solution has been found for parametrically excited vibrations simultaneously occurring in both planes (modes y_q and z_q) (except when there is perfect tuning of these two modes, which occurs for even q or a taut string, in which case the plane of the parametrically excited response is arbitrary). Similarly no solution for simultaneous steady state responses in modes y_q and z_q was found by numerical continuation of averaged modulation equations similar to Eqs. (3)–(6) by Marsico *et al.* [33] nor of cable equations of motion similar to Eqs. (1) and (2) by Massow [39], so it is possible that no such solution exists.

4. Stability of solutions

The stability of all the solutions is considered by expanding Eqs. (3)–(6) for modes y_p, z_p, y_q and z_q (or modes y_p and z_p only if p is odd so modes y_q and z_q do not exist), with $\tilde{y}_{nc}=y_{nc0}+y_{nc1}$, etc., where y_{nc0} is the solution and y_{nc1} is a small perturbation. Retaining only linear terms in the perturbations, the modulation equations for the perturbations can be expressed in matrix form as

$$\mathbf{x}_1' = \mathbf{G}\mathbf{x}_1 \tag{39}$$

where $\mathbf{x}_1=\{y_{pc1}\ y_{ps1}\ z_{pc1}\ z_{ps1}\ y_{qc1}\ y_{qs1}\ z_{qc1}\ z_{qs1}\}^{\mathrm{T}}$ and $\mathbf{G}$ can be expressed as

$$\mathbf{G}=\mathbf{G_0}+\mathbf{G_{1A}}\mathbf{G_{1B}} \tag{40}$$

where

$$\mathbf{G_0}=\frac{\varepsilon\omega_p}{2}\begin{bmatrix} -2\xi_{yp} & -2b_{yp0} & 0 & 2c_{p0} & 0 & 0 & 0 & 0 \\ 2b_{yp0} & -2\xi_{yp} & -2c_{p0} & 0 & 0 & 0 & 0 & 0 \\ 0 & 2c_{p0} & -2\xi_{zp} & -2b_{zp0} & 0 & 0 & 0 & 0 \\ -2c_{p0} & 0 & 2b_{zp0} & -2\xi_{zp} & 0 & 0 & 0 & 0 \\ 0 & 0 & 0 & 0 & -\xi_{yq} & -b_{yq0}-U_0 & 0 & c_{q0} \\ 0 & 0 & 0 & 0 & b_{yq0}-U_0 & -\xi_{yq} & -c_{q0} & 0 \\ 0 & 0 & 0 & 0 & 0 & c_{q0} & -\xi_{zq} & -b_{zq0}-U_0 \\ 0 & 0 & 0 & 0 & -c_{q0} & 0 & b_{zq0}-U_0 & -\xi_{zq} \end{bmatrix}$$

$$c_{n0}=\frac{1}{16\varepsilon_s}\tilde{C}_{n0},\ U_0=\frac{1}{4\varepsilon_s(1+\lambda^2/12)}\hat{U},$$

$$\mathbf{G_{1A}}=\frac{\varepsilon\omega_p}{2}\begin{bmatrix} 2y_{ps0} & 0 & 0 & 0 & 2z_{ps0} & 0 \\ -2y_{pc0} & 0 & 0 & 0 & -2z_{pc0} & 0 \\ 0 & 2z_{ps0} & 0 & 0 & 2y_{ps0} & 0 \\ 0 & -2z_{pc0} & 0 & 0 & -2y_{pc0} & 0 \\ 0 & 0 & y_{qs0} & 0 & 0 & z_{qs0} \\ 0 & 0 & -y_{qc0} & 0 & 0 & -z_{qc0} \\ 0 & 0 & 0 & z_{qs0} & 0 & y_{qs0} \\ 0 & 0 & 0 & -z_{qc0} & 0 & -y_{qc0} \end{bmatrix},$$

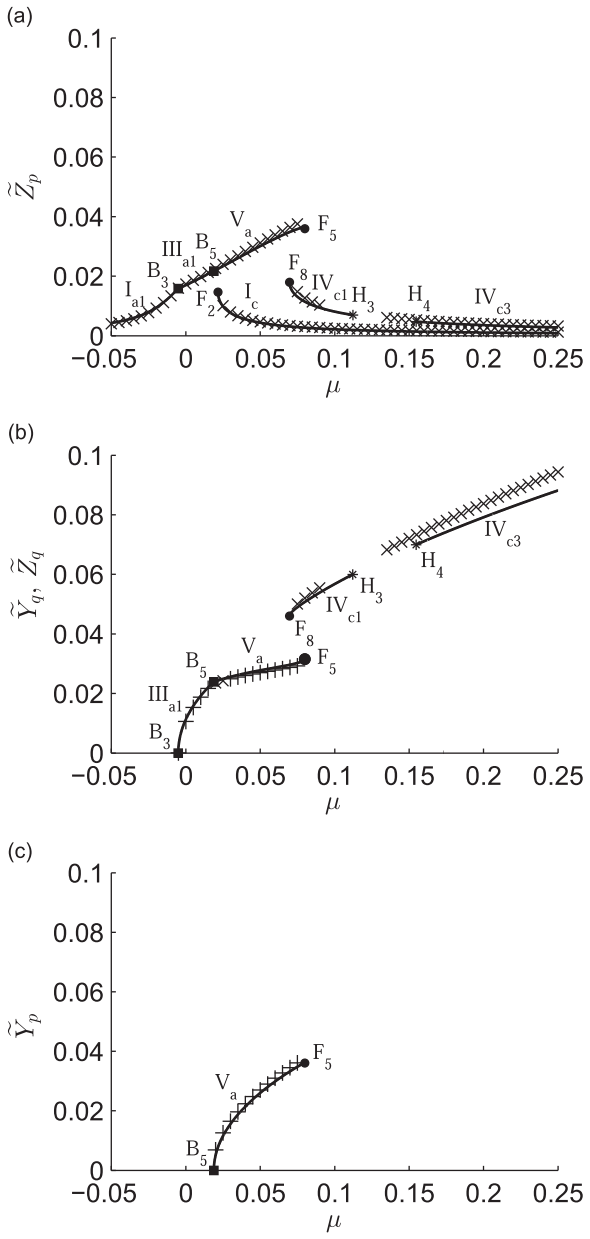

Fig. 10. Frequency response curves of modes z_p (a), y_q and z_q (b) and y_p (c) for the cable in Table 1 for excitation with $p=2$ for input amplitude $\hat{\Delta} = 0.25 \times 10^{-3}$. Curves show stable branches from Figs. 6 and 8, with symbols as for Fig. 2. Crosses indicate steady state solutions from time history simulations of Eqs. (1) and (2); $\times$, z-plane response; $+$, y-plane response. Zero amplitude responses are omitted for clarity.

$$\mathbf{G_{1B}} = \frac{1}{16\varepsilon_s}\begin{bmatrix} 3y_{pc0} & 3y_{ps0} & z_{pc0} & z_{ps0} & 2y_{qc0} & 2y_{qs0} & 2z_{qc0} & 2z_{qs0} \\ y_{pc0} & y_{ps0} & 3z_{pc0} & 3z_{ps0} & 2y_{qc0} & 2y_{qs0} & 2z_{qc0} & 2z_{qs0} \\ 2y_{pc0} & 2y_{ps0} & 2z_{pc0} & 2z_{ps0} & 3y_{qc0} & 3y_{qs0} & z_{qc0} & z_{qs0} \\ 2y_{pc0} & 2y_{ps0} & 2z_{pc0} & 2z_{ps0} & y_{qc0} & y_{qs0} & 3z_{qc0} & 3z_{qs0} \\ z_{pc0} & z_{ps0} & y_{pc0} & y_{ps0} & 0 & 0 & 0 & 0 \\ 0 & 0 & 0 & 0 & z_{qc0} & z_{qs0} & y_{qc0} & y_{qs0} \end{bmatrix}. \tag{}$$

The solution is stable if the real parts of all the eigenvalues of the matrix **G** are negative. So, having found the steady state solutions from the polynomials in Section 3, the stability of each solution is determined numerically from the eigenvalues of **G** (or its top left 4×4 sub-matrix if p is odd so modes y_q and z_q do not exist).

Modulated responses are initiated if any eigenvalues of **G** have a positive real part and non-zero imaginary part. Such solutions are bounded by Hopf bifurcations.

5. Numerical and experimental validation

The results of the analytical solutions of the vibration amplitudes given in Section 3 have been validated by numerical integration of the equations of motion, Eqs. (1) and (2), using the Runge–Kutta (4,5) method implemented in Matlab®. 12 modes were included in each plane, to allow for possible modal interactions beyond those covered by the averaging analysis, in particular those associated with the quadratic nonlinearities, involving asymmetry of the effective stiffness due to the sag and components of response equivalent to the distortion of the actual mode shapes. Obviously the modal responses were not constrained to be near their natural frequencies (c.f. assumption (vii) in Section 2.3). For comparison with the earlier results, the same parameters of the cable and the input were used as for Figs. 6 and 8, i.e. for vertical in-plane excitation of the lower anchorage around the 2nd natural frequency.

Many sets of initial conditions were defined, based on the analytical solutions, including both stable and unstable branches, and also for points beyond the predicted folds and other arbitrary initial conditions. All modes with zero response predicted by the averaging were given initial conditions of displacement and velocity equal to 1/100th of the initial conditions for the directly excited mode, z_p, to give vibrations in those modes the opportunity to develop.

The steady state amplitudes from the numerical simulations are plotted as crosses in Fig. 10, along with the stable solutions from the analytical solutions in Figs. 6 and 8, represented by curves. As can be seen there is excellent agreement of the results, especially for solutions I, III and V. All of the predicted stable solutions, and no others, have been found. The maximum error in the predicted non-zero amplitudes in solutions I, III and V is 4.8% of the maximum amplitude in the directly excited mode (z_p). In Fig. 10 there are no stable branches for solution II, but similarly good results were found for this solution for the cases in Figs. 2 and 4.

In Fig. 10 the only significant discrepancies are for solution IV as the detuning of the excitation frequency μ increases above 0.1. This is not unexpected since the accuracy of the approximation in the averaging (assumption (vi) in Section 2.3) decreases as the detuning of the excitation frequency increases. For $\mu=0.25$ the error in the estimated amplitude of the parametrically excited mode in solution IV is 6.6% (or 17% of the maximum amplitude of mode z_p). The predicted break in the stable solutions on branch IV_c between the Hopf bifurcations H_3 and H_4 was found from the numerical simulations, albeit for a lower range of μ. Within this range the numerical simulations either exhibited quasi-periodic or apparently chaotic responses, as expected, or converged on the stable solution branch I_c.

For the modes with zero predicted amplitude from the averaging analysis, the amplitudes from the numerical simulations were always small so the results are not plotted for clarity. The maximum amplitude of any of these modes for $|\mu|<0.1$ was 1.4% of the maximum amplitude of mode z_p, rising to 2.5% for $\mu=0.25$. Therefore, although clearly including these modes gives refined results, it seems that for typical taut cables the reduction to a maximum of four participating modes in the averaging analysis is reasonable.

In terms of validation against experiments, solution I was previously found to match the measurements from a scaled physical model of a bridge stay-cable [35], including the effect of the axial component of the excitation. The turning points of solution I and the bifurcations to solutions III and IV also matched experiments well [32,35]. Unfortunately the responses after the bifurcations were not investigated in the experiments. However, for a taut string, Nayfeh et al. [24] did experimentally and numerically identify the steady state responses in what are defined here as solutions I, II, IV and VI (solutions III and V were not distinguished from IV and VI respectively, since, in the absence of sag, modes y_q and z_q were reduced to only one DOF). Using their parameter values (which convert to $\varepsilon_s=0.0356$, $\Gamma=0.190$, $\theta=90^\circ$, $\lambda^2=0$, $\xi_{y6}=\xi_{z6}=0.092\%$, $\xi_{y3}=0.088\%$, with excitation around the natural frequency of the 6th mode pair), the analytical expressions given here are able to reproduce their plots, obtained by numerical continuation, for all the solutions, for both stable and unstable branches. Their experiments showed good agreement with their numerical results for stable solutions, for three different amplitudes of transverse excitation and two other orientations of end motions with respect to the axis of the string. Hence the proposed analytical solutions are validated against their experiments for a taut string, with very different parameter values from the example cable considered otherwise in this paper (Table 1). The advantages of the current analysis over that of Nayfeh et al. [24] are the solutions being in the form of analytical (polynomial) expressions and that they can account for the important effects of very small sag.

6. Conclusions

The steady state multi-modal vibration amplitudes of taut cables subject to dynamic excitation have been addressed. The cable model adopted allows for cable inclination, small sag (with $\lambda^2 \leq O(1)$), which causes differences in behaviour in the two transverse planes, an infinite number of nonlinearly coupled modes in both planes, and excitation, from cable end motion (with components along and normal to the cable) and/or external forcing, close to any natural frequency. The method of scaling and averaging has been used to derive modulation equations for the cable response in each mode (Eqs. (3)–(6)) and hence a set of non-dimensional nonlinear algebraic equations for the steady state responses (Eqs. (7)–(10)). It has been shown that, on this basis, for positive damping and planar excitation close to any natural frequency, steady state responses can only occur in up to four modes: the directly excited mode, the corresponding mode in the orthogonal plane (with close to the same natural frequency) through nonlinear coupling and, when the excitation frequency is close to that of

an even numbered mode and there is a component of end motion axial to the cable, in the two modes with nominally half the natural frequency through parametric excitation.

The main contribution of this work is to provide analytical expressions for the steady state vibration amplitudes in each of six solutions involving different combinations of modes, in the form of a single polynomial equation for each solution. Previously the only analytical solution allowing for the sag was for solution I (i.e. the directly excited mode only) [32], whilst for a taut string (i.e. no sag) there were solutions for certain other specific cases involving one or two modes [10,11,13,14,20,25,26]. All other previous solutions of the response amplitudes have been numerical, normally using time history simulations or numerical continuation. The proposed analytical solutions allow for sag (though very small), different damping ratios in each mode, excitation around any natural frequency, and inputs at both ends with components both axial and transverse to the cable. As non-dimensional polynomials they can be easily applied to any taut cable to find the response amplitude in each mode, and the number of solutions is known so none will be missed. No steady state solutions have been found with responses in both planes simultaneously in the potentially primary parametrically excited modes (i.e. at half the natural frequency) – it may be that no such steady state solutions exist – but solutions have been presented for all other possible combinations of modal responses (within the limitations of the assumptions), i.e. for up to three modes.

Another key novel finding is the effect of very small sag on the nonlinear dynamic behaviour of cables. Although the analysis is limited to cables that are close to a taut string ($\lambda^2 \leq O(1)$), the difference is important. The detuning of the first in-plane mode due to the very small sag re-stabilises the top of the upper branch of solution I and the top section of solution II (e.g. see Fig. 4 c.f. Fig. 2 for only 0.225% detuning) and the sag-related direct excitation from the axial component of end motion is also important (e.g. see Fig. 5 c.f. Fig. 4 for the same detuning). Furthermore the very small sag determines the plane in which parametrically excited vibrations occur (e.g. see Figs. 6, 7 and 10).

One other specific finding from the analytical solutions is that when a mode is parametrically excited its amplitude is always reduced by the presence of the directly excited mode.

The derived equations have been validated by comparing the results with those from direct numerical integration of the equations of motion including 24 modes. Excellent agreement has been found for when the detuning of the excitation frequency from a natural frequency is small ($< 10\%$), with errors gradually increasing thereafter. It has been confirmed that the responses in modes other than the four covered by the analytical solutions are unimportant. The results are also consistent with previous results from numerical continuation and experiments for the simplified case of a taut string.

Acknowledgement

Part of this work was conducted under an EPSRC Advanced Research Fellowship (No. EP/D073944/1).

References

[1] A.H. Nayfeh, P.F. Pai, *Linear and Nonlinear Structural Mechanics*, Wiley, 2004.
[2] G. Rega, Nonlinear vibrations of suspended cables – Part1: Modeling and analysis, *Applied Mechanics Review* 57 (6) (2004) 443–478.
[3] G. Rega, Nonlinear vibrations of suspended cables – Part II: Deterministic phenomena, *Applied Mechanics Review* 57 (6) (2004) 479–514.
[4] R.A. Ibrahim, Nonlinear vibrations of suspended cables – Part III: Random excitation and interaction with fluid flow, *Applied Mechanics Review* 57 (6) (2004) 515–549.
[5] H.M. Irvine, T.K. Caughey, The linear theory of free vibrations of a suspended cable, *Proceedings of the Royal Society of London A* 341 (1974) 299–315.
[6] N.C. Perkins, Modal interactions in the non-linear response of elastic cables under parametric/external excitation, *International Journal of Non-Linear Mechanics* 27 (2) (1992) 233–250.
[7] C. Lee, N.C. Perkins, Three-dimensional oscillations of suspended cables involving simultaneous internal resonances, *Nonlinear Dynamics* 8 (1) (1995) 45–63.
[8] F. Benedettini, G. Rega, R. Alaggio, Non-linear oscillations of a four-degree-of-freedom model of a suspended cable under multiple internal resonance conditions, *Journal of Sound and Vibration* 182 (5) (1995) 775–798.
[9] G. Rega, W. Lacarbonara, A.H. Nayfeh, C.M. Chin, Multiple resonances in suspended cables: direct versus reduced-order models, *International Journal of Non-linear Mechanics* 34 (5) (1999) 901–924.
[10] SETRA, Cable Stays; *Recommendations of French Interministerial Commission on Prestressing*, Center des Techniques des Ouvraes d'Art, Bagneux Cedex, France, 2002.
[11] E. Caetano, *Cable Vibrations in Cable-Stayed Bridges*, Structural Engineering Document 9, International Association for Bridge and Structural Engineering (IABSE), Zurich, 2007.
[12] V. Gattulli, M. Lepidi, Nonlinear interactions in the planar dynamics of cable-stayed beam, *International Journal of Solids and Structures* 40 (18) (2003) 4729–4748.
[13] A.H. Nayfeh, D.T. Mook, *Nonlinear Oscillations*, Wiley, 1979.
[14] J. Miles, Resonant, nonplanar motion of a stretched string, *The Journal of the Acoustical Society of America* 75 (1984) 1505–1510, http://dx.doi.org/10.1121/1.390821.
[15] A.K. Bajaj, J.M. Johnson, On the amplitude dynamics and crisis in resonant motion of stretched strings, *Philosophical Transactions of the Royal Society London A* 338 (1992) 1–41, http://dx.doi.org/10.1098/rsta.1992.0001.
[16] F. Benedettini, G. Rega, Non-linear dynamics of an elastic cable under planar excitation, *International Journal of Non-Linear Mechanics* 22 (6) (1987) 497–509.
[17] V. Gattulli, L. Martinelli, F. Perotti, F. Vestroni, Nonlinear oscillations of cables under harmonic loading using analytical and finite element models, *Computer Methods in Applied Mechanics and Engineering* 193 (1–2) (2004) 69–85.
[18] N. Srinil, G. Rega, S. Chucheepsakul, Two-to-one resonant multi-modal dynamics of horizontal/inclined cables. Part I: theoretical formulation and model validation, *Nonlinear Dynamics* 48 (2007) 231–252.

[19] N. Srinil, G. Rega, Two-to-one resonant multi-modal dynamics of horizontal/inclined cables. Part II: internal resonance activation, reduced-order models and nonlinear normal modes, *Nonlinear Dynamics* 48 (2007) 253–274.
[20] G. Tagata, Harmonically forced, finite amplitude vibration of a string, *Journal of Sound and Vibration* 51 (4) (1977) 483–492.
[21] R. Uhrig, On kinetic response of cables of cable-stayed bridges due to combined parametric and forced excitation, *Journal of Sound and Vibration* 165 (1) (1993) 185–192.
[22] J.L. Lilien, A. Pinto da Costa, Vibration amplitudes caused by parametric excitation of cable-stayed structures, *Journal of Sound and Vibration* 174 (1) (1994) 69–90.
[23] Y. Cai, S.S. Chen, Dynamics of elastic cable under parametric and external resonances, *ASCE Journal of Engineering Mechanics* 120 (8) (1994) 1786–1802.
[24] S.A. Nayfeh, A.H. Nayfeh, D.T. Mook, Nonlinear response of a taut string to longitudinal and transverse end excitation, *Journal of Vibration and Control* 1 (1995) 307–334.
[25] A. Pinto da Costa, J. Martins, F. Branco, J.L. Lilien, Oscillations of bridge stay cables induced by periodic motions of deck and/or towers, *ASCE Journal of Engineering Mechanics* 122 (1996) 613–622.
[26] Caswita, A.H.P. Van Der Burgh, Combined parametrical transverse and in-plane harmonic response of an inclined stretched string, *Journal of Sound and Vibration* 267 (4) (2003) 913–931, http://dx.doi.org/10.1016/S0022-460X(03)00252-9.
[27] A. Berlioz, C.-H. Lamarque, A non-linear model for the dynamics of an inclined cable, *Journal of Sound and Vibration* 279 (3–5) (2005) 619–639.
[28] C.T. Georgakis, C.A. Taylor, Nonlinear dynamics of cable stays. Part 1: sinusoidal cable support excitation, *Journal of Sound and Vibration* 281 (2005) 537–564.
[29] C.T. Georgakis, C.A. Taylor, Nonlinear dynamics of cable stays. Part 2: stochastic cable support excitation, *Journal of Sound and Vibration* 281 (2005) 565–591.
[30] L. Wang, Y. Zhao, Large amplitude motion mechanism and non-planar vibration character of stay cables subject to the support motions, *Journal of Sound and Vibration* 327 (1-2) (2009) 121–133.
[31] A. Gonzalez-Buelga, S.A. Neild, D.J. Wagg, J.H.G. Macdonald, Modal stability of inclined cables subjected to vertical support excitation, *Journal of Sound and Vibration* 318 (3) (2008) 565–579, http://dx.doi.org/10.1016/j.jsv.2008.04.031.
[32] J.H.G. Macdonald, M.S. Dietz, S.A. Neild, A. Gonzalez-Buelga, A.J. Crewe, D.J. Wagg, Generalised modal stability of inclined cables subjected to support excitations, *Journal of Sound and Vibration* 329 (21) (2010) 4515–4533, http://dx.doi.org/10.1016/j.jsv.2010.05.002.
[33] M.R. Marsico, V. Tzanov, D.J. Wagg, S.A. Neild, B. Krauskopf, Bifurcation analysis of a parametrically excited inclined cable close to two-to-one internal resonance, *Journal of Sound and Vibration* 330 (2011) 6023–6035, http://dx.doi.org/10.1016/j.jsv.2011.07.027.
[34] P. Warnitchai, Y. Fujino, T. Susumpow, A nonlinear dynamic model for cables and its application to a cable structure-system, *Journal of Sound and Vibration* 187 (4) (1995) 695–712.
[35] J.H.G. Macdonald, M.S. Dietz, S.A. Neild, Dynamic excitation of cables by deck and/or tower motion, *Proceedings of ICE: Bridge Engineering* 163 (BE2) (2010) 101–111, http://dx.doi.org/10.1680/bren.2010.163.2.101.
[36] M.J. Ernst, Der E-Modul von Seilen unter Berücksichtigung des Derchhanges (The E-modulus of cables taking into account their sag), *Der Bauingenieur* 40 (2) (1965) 52–55.
[37] J.H.G. Macdonald, Separation of the contributions of aerodynamic and structural damping in vibrations of inclined cables, *Journal of Wind Engineering and Industrial Aerodynamics* 90 (1) (2002) 19–39, http://dx.doi.org/10.1016/S0167-6105(01)00110-6.
[38] T. Bakri, R. Nabergoj, A. Tonel, F. Verhulst, Parametric excitation in non-linear dynamics, *International Journal of Non-linear Mechanics* 39 (2004) 311–329.
[39] C.L.S. Massow, Bifurcation and Numerical Integration Analysis of Parametric Excitation of Inclined Cables, PhD Thesis, University of Bristol, 2010.